IMAGE DATABASES IN MEDICAL APPLICATIONS

Doctoral Dissertation

Juha Koikkalainen

Helsinki University of Technology
Department of Engineering Physics and Mathematics
Laboratory of Biomedical Engineering

IMAGE DATABASES IN MEDICAL APPLICATIONS
Doctoral Dissertation

Juha Koikkalainen

Dissertation for the degree of Doctor of Science in Technology to be presented with due permission of the Department of Engineering Physics and Mathematics for public examination and debate in Auditorium F1 at Helsinki University of Technology (Espoo, Finland) on the 17th of March, 2006, at 12 noon.

Helsinki University of Technology
Department of Engineering Physics and Mathematics
Laboratory of Biomedical Engineering

Teknillinen korkeakoulu
Teknillisen fysiikan ja matematiikan osasto
Lääketieteellisen tekniikan laboratorio

HELSINKI UNIVERSITY OF TECHNOLOGY
P. O. BOX 1000, FI-02015 TKK
http://www.tkk.fi

ABSTRACT OF DOCTORAL DISSERTATION

Author	Juha Koikkalainen

Name of the dissertation
Image Databases in Medical Applications

Date of manuscript	October 18, 2005	Date of the dissertation	March 17, 2006

☐ Monograph ☒ Article dissertation (summary + original articles)

Department	Department of Engineering Physics and Mathematics
Laboratory	Laboratory of Biomedical Engineering
Field of research	Medical image processing
Opponent(s)	Ass. Prof., Head of Laboratory Alejandro Frangi (Pompeu Fabra University)
Supervisor	Acting Professor Risto Ilmoniemi (Helsinki University of Technology)
(Instructor)	Docent Jyrki Lötjönen (VTT Technical Research Centre of Finland)

Abstract

The number of medical images acquired yearly in hospitals increases all the time. These imaging data contain lots of information on the characteristics of anatomical structures and on their variations. This information can be utilized in numerous medical applications. In deformable model-based segmentation and registration methods, the information in the image databases can be used to give *a priori* information on the shape of the object studied and the gray-level values in the image, and on their variations. On the other hand, by studying the variations of the object of interest in different populations, the effects of, for example, aging, gender, and diseases on anatomical structures can be detected.

In the work described in this Thesis, methods that utilize image databases in medical applications were studied. Methods were developed and compared for deformable model-based segmentation and registration. Model selection procedure, mean models, and combination of classifiers were studied for the construction of a good *a priori* model. Statistical and probabilistic shape models were generated to constrain the deformations in segmentation and registration so that only the shapes typical to the object studied were accepted. In the shape analysis of the striatum, both volume and local shape changes were studied. The effects of aging and gender, and also the asymmetries were examined.

The results proved that the segmentation and registration accuracy of deformable model-based methods can be improved by utilizing the information in image databases. The databases used were relatively small. Therefore, the statistical and probabilistic methods were not able to model all the population-specific variation. On the other hand, the simpler methods, the model selection procedure, mean models, and combination of classifiers, gave good results also with the small image databases. Two main applications were the reconstruction of 3-D geometry from incomplete data and the segmentation of heart ventricles and atria from short- and long-axis magnetic resonance images. In both applications, the methods studied provided promising results. The shape analysis of the striatum showed that the volume of the striatum decreases in aging. Also, the shape of the striatum changes locally. Asymmetries in the shape were found, too, but any gender-related local shape differences were not found.

Keywords	medical image processing, deformable-models, statistical and probabilistic shape models, shape analysis

Tiivistelmä

Sairaaloissa otettavien lääketieteellisten kuvien määrä kasvaa vuosittain. Tämä kuvantamisdata sisältää runsaasti informaatiota anatomisten kohteiden ominaispiirteistä ja niiden varioinnista. Tätä informaatiota voidaan hyödyntää useissa lääketieteellisissä sovelluksissa. Muotoutuviin malleihin perustuvissa segmentointi- ja kohdennusmenetelmissä kuvatietokantojen sisältämää informaatiota voidaan käyttää antamaan etukäteistietoa tutkittavan kohteen muodosta, kuvien harmaasävyarvoista ja näiden varioinnista. Toisaalta tutkimalla kohteiden muotojen variointia eri populaatioissa voidaan tutkia esimerkiksi ikääntymisen, sukupuolen ja tautien vaikutusta.

Tässä väitöskirjassa tutkittiin eri menetelmiä, joilla kuvatietokantoja voidaan käyttää lääketieteellisissä sovelluksissa. Työssä kehitettiin ja verrattiin menetelmiä muotoutuviin malleihin perustuvaan kuvien segmentointiin ja kohdentamiseen. A priori-mallien muodostamiseksi tutkittiin mallinvalintamenetelmää, keskiarvomalleja ja luokittelutulosten yhdistämistä. Tilastollisia ja todennäköisyysteoreettisia menetelmiä käytettiin muotoutumisen rajoittamisessa siten, että sallittiin vain tutkittavalle kohteelle tyypilliset muotoutumiset. Striatumin muotoanalyysissä tutkittiin sekä tilavuusmuutoksia että lokaaleja muodonmuutoksia ikääntymisessä ja sukupuolten välillä. Myös striatumin asymmetriaa tutkittiin.

Väitöskirjan tulokset osoittavat, että hyödyntämällä kuvatietokannoissa olevaa informaatiota voidaan muotoutuviin malleihin perustuvissa menetelmissä parantaa segmentointi- ja kohdennustarkkuutta. Työssä käytettyjen kuvatietokantojen koko oli niin pieni, että tilastolliset ja todennäköisyysteoreettiset menetelmät eivät kyenneet täysin mallintamaan tutkittavien kohteiden variaatiota. Toisaalta yksinkertaisemmat menetelmät, eli mallinvalinta, keskiarvomallit ja luokitteluiden yhdistäminen, antoivat hyviä tuloksia myös pienillä kuvatietokannoilla. Menetelmien soveltaminen keskittyi kahteen ongelmaan: 3-D geometrian rekonstruktio harvasta pistejoukousta ja sydämen kammioiden ja eteisten segmentointi käyttäen sekä lyhyen- että pitkänakselin magneettiresonanssikuvia. Näissä sovelluskohteissa tutkitut menetelmät antoivat lupaavia tuloksia. Striatumin muotoanalyysin tulokset osoittivat, että striatumin tilavuus pienenee iän funktiona. Samalla striatumin muoto muuttuu lokaalisti. Toisaalta lokaaleja muotoeroja ei havaittu miesten ja naisten välillä. Lisäksi tutkimuksessa havaittiin asymmetrioita striatumin muodossa.

Preface

The research for this thesis was carried out mostly at the Laboratory of Biomedical Engineering, Helsinki University of Technology, and at the Institute of Signal Processing, Tampere University of Technology, and Turku PET Center. The work was carried out as a part of the graduate school Functional Imaging in Medicine, the Academy of Finland's center of excellence Helsinki Brain Research Center (HBRC), and as a part of several National Technology Agency of Finland (TEKES) funded projects.

I wish to thank my former supervisor and the Head of the Laboratory of Biomedical Engineering, Professor (emer.) Toivo Katila, for the possibility to do my research, for all the comments during my research, and the excellent working environment in the image processing group. In addition, I wish to thank Acting Professor Risto Ilmoniemi, the supervisor of the Thesis, for his comments on the Thesis. I am grateful to professor Ulla Ruotsalainen and professor Jarmo Hietala for the opportunity to work in their groups and for their ideas and comments. Above all, I would like to thank docent Jyrki Lötjönen, the instructor of the Thesis, for many research ideas, comments, and support during all these years.

I am grateful to the preliminary examiners, professor Daniel Rueckert and professor Heikki Kälviäinen, for their comments on the manuscript. Also, I would like to thank the co-authors, docent Kirsi Lauerma, MD Sari Kivistö, MD Mikko Nyman, PhD Tim Cootes, M.Sc. Mika Pollari, M.Sc. Kari Antila, M.Sc. Elina Lamminmäki, M.Sc. Daniel Smutek, and Mr. Mikko Lilja, for their valuable contribution. I wish to thank docent Mark van Gils for the proof-reading of the thesis.

I have been privileged as I have had the opportunity to work in the Laboratory of Biomedical Engineering, Helsinki University of Technology. I would like to thank all the personnel and colleagues in the laboratory for the great atmosphere. Especially, I wish to thank all the former and present members of the image processing group, D.Sc. Timo Mäkelä, M.Sc. Mika Pollari, M.Sc. Henrik Lohman, Mr. Henri Veisterä, Mr. Mikko Lilja, and Mr. Tuomas Tölli, for all the conversations, comments, and help.

The financial support provided by the Finnish Cultural Foundation, the Jenny and Antti Wihuri Foundation, and the Research Foundation of Helsinki University of Technology is gratefully acknowledged.

Finally, I want to express my gratitude to my parents and brothers, and all the relatives and friends for their support and encouragement. Last, but certainly not least, I thank my fiancée Riitta for her support, patience, and encouragement during this work.

Tampere, February 2006

Juha Koikkalainen

Contents

List of publications

This Thesis consists of an overview and of the following seven publications:

I Koikkalainen, J. and Lötjönen, J. (2004). Reconstruction of 3-D Head Geometry from Digitized Point Sets: An Evaluation Study. *IEEE Transactions on Information Technology in Biomedicine*, 8(3):377–386.

II Lötjönen, J., Kivistö, S., Koikkalainen, J., Smutek, D., and Lauerma K. (2004). Statistical Shape Model of Atria, Ventricles and Epicardium from Short- and Long-Axis MR Images. *Medical Image Analysis*, 8(3):371–386.

III Koikkalainen, J., Nyman, M., Hietala, J., Lötjönen, J., and Ruotsalainen U. (2005). Age- and Gender-Related Shape Changes and Asymmetry of Striatum. *Helsinki University of Technology, Publications in Engineering Physics*, Report A839 (TKK-F-A839).

IV Koikkalainen, J., Pollari, M., Lötjönen, J., Kivistö, S., and Lauerma, K. (2004). Segmentation of Cardiac Structures Simultaneously from Short- and Long-Axis MR Images. In Barillot, C., Haynor, D. R., and Hellier, P., editors, *MICCAI (1)*, volume 3216 of *Lecture Notes in Computer Science*, pages 427–434. Springer.

V Lötjönen, J., Antila, K., Lamminmäki, E., Koikkalainen, J., Lilja, M., and Cootes, T. F. (2005). Artificial Enlargement of a Training Set for Statistical Shape Models: Application to Cardiac Images. In Frangi, A. F., Radeva, P., Santos, A., and Hernandez, M., editors, *FIMH*, volume 3504 of *Lecture Notes in Computer Science*, pages 92–101. Springer.

VI Koikkalainen, J. and Lötjönen, J. (2003). Individualized Geometric Model from Unorganized 3-D Points: An Application to Thorax Modeling. In Ellis, R. E. and Peters, T. M., editors, *MICCAI (1)*, volume 2878 of *Lecture Notes in Computer Science*, pages 91–98. Springer.

VII Koikkalainen, J. and Lötjönen, J. (2002). Model Library for Deformable Model-Based Segmentation of 3-D Brain MR-Images. In Dohi, T. and Kikinis, R., editors, *MICCAI (1)*, volume 2488 of *Lecture Notes in Computer Science*, pages 540–547. Springer.

Throughout the overview, these publications are referred to by the roman numerals indicated above.

List of abbreviations and symbols

1-,2-,3-,4-D	One-, two-, three-, four-dimensional
ASM	Active shape model
DBM	Deformation-based morphometry
FFD	Free-form deformation
ICA	Independent component analysis
LA	Long-axis
MAP	Maximum *a posteriori*
MRI	Magnetic resonance imaging
NMI	Normalized mutual information
PCA	Principal component analysis
PDF	Probability density function
PDM	Point distribution model
SA	Short-axis
SDM	Statistical deformation model
TRE	Target registration error
VBM	Voxel-based morphometry
d	Dimension of space
$\mathbf{d}(x, y, z)$	Deformation of point
$\mathbf{I}(x, y, z)$	Intensity of gray-level image
N	Size of database
n	Number of shape parameters
$\mathbf{T}(x, y, z)$	Transformation of point
$\mathbf{x}$	Parametrization of shape

1 Introduction

In the 19th century, it was assumed that the personality of a human can be inferred from the shape of a skull. The shape of a skull was used to study racial theories and intelligence, too. Also the shape of other parts of the human body were used to assess personality. For example, criminals were identified based on facial features or long hands. The most horrific example of the racial segregation based on the shape of human body is from nazi Germany, where the humans were classified based on the shape of body parts to create a "superior" Aryan race.

The shape of human body parts and organs has always been used in medicine. Nowadays, modern medical imaging modalities provide accurate information on the anatomy of the human body. Traditionally, physicians make diagnoses based on visual examination of the imaging data. They have many years of experience with the appearance of imaging data and they have learned how the appearance varies. If a senior physician cannot represent the learned knowledge on the appearance of the data in a well-defined and constructive way, this experience cannot be passed on to younger physicians, and lots of valuable information that could be used in future diagnoses would be lost. For example, it is very difficult to assess the normality of the striatum, a group of nuclei in the brain, by visually studying the imaging data of an individual (Fig. 1a). A more reliable diagnosis is obtained by comparing the data to the corresponding imaging data of a reference subject who is known to be healthy (Fig. 1b). Even better, the comparison can be performed utilizing the imaging data of many healthy individuals (Fig. 1c). The normal variations among healthy people can be quantified from the imaging data of healthy individuals, and the differences that indicate the existence of a disease can be detected more reliably, and a false diagnosis may be avoided.

In this Thesis, methods were studied to capture diagnostically important information from the imaging data of a group of individuals and to utilize this information in different medical applications. The focus was on image databases, from which the information on the shapes and appearances of the objects and their variability could be extracted and modeled. These computational methods enable the storage of the information on the variability in the imaging data, and may help physicians to perform more reliable and objective diagnoses.

| (a) | (b) | (c) |
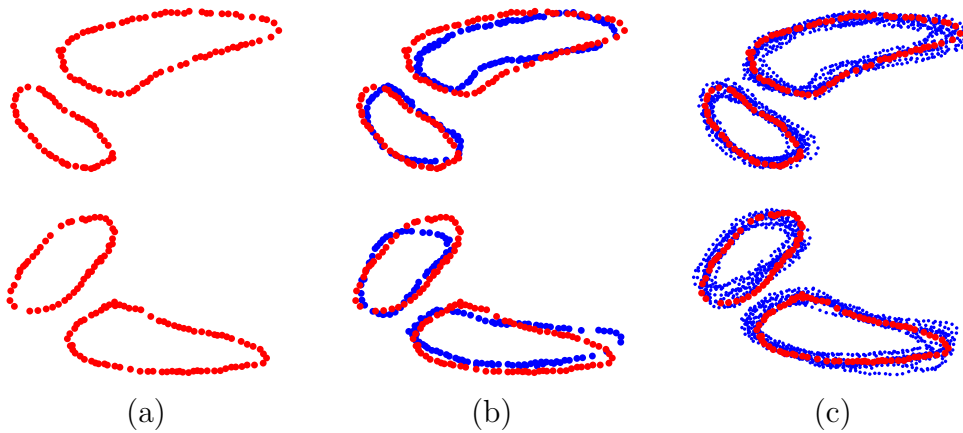
Figure 1: Visual assessment of the normality of a shape. (a) The shape of the striatum of an individual. The normality of the shape is difficult to assess. (b) The shape is compared to a reference shape from the population of healthy people. Obvious shape differences exist, but it is difficult to say if these differences are normal inter-subject variations. (c) The comparison is done using 11 reference shapes. Now, it is seen that the shape studied is within the normal inter-subject shape variation, and the shape can be classified as a normal case.

1.1   Modeling and utilization of prior knowledge

The number of medical images acquired yearly in hospitals increases, but the physicians have only limited time to examine these data. Only qualitative information can be obtained from the images if only visual examination is used. However, quantitative information on the size and shape of the anatomical structures is needed for better diagnosis of patients. Quantitative information can be retrieved using manual methods, but they are usually time-consuming. In addition, the results of manual methods are not objective because of the differences in the experience and routines of the physicians. Based on these facts, it is obvious that automatic methods to analyze medical imaging data are needed to give objective quantitative information and to save the workload of physicians.

Each time quantitative information from imaging data is needed, image segmentation has to be performed. In image segmentation, an image is divided into parts that represent real world objects and regions that are visible in the image. Although this task is relatively easy for human eye, it has been surprisingly difficult to implement a universal automatic segmentation algorithm, mainly because of noise, occlusion, incomplete data, and other structures in images. For example, contours of the object of interest are often discontinuous, and the automatic segmentation algorithm has to estimate the location of the missing contours from the other data in the image or from prior knowledge on the problem. Therefore, image segmentation is still one of the most studied topics in medical image analysis.

Image segmentation methods are usually designed for some particular application. The application-specific methods enable the complete utilization of prior knowledge about the problem. For example, the shapes of most anatomical objects have only a restricted anatomical variability. Therefore, strong prior information on the location, shape, and appearance of the objects is available. The use of such prior knowledge is especially important when data are noisy and incomplete.

Deformable model-based segmentation methods are popular in medical applications (Kass et al., 1987; McInerney and Terzopoulos, 1996; Archarya and Menon, 1998; Dawant and Zijdenbos, 2000; Xu et al., 2000a; Rogowska, 2001; Maintz and Viergever, 1998; Fitzpatrick et al., 2000; Hawkes, 2001; Rueckert, 2001; Hill and Batchelor, 2001; Mäkelä et al., 2002). The most attractive feature in these methods is that many kinds of prior information can be effectively utilized. The basic idea in deformable model-based segmentation methods is to deform iteratively an *a priori* model in such a way that it matches to the target data (i.e., imaging data of subject to be segmented) as accurately as possible. An *a priori* model is usually a gray-level image or a surface that represents the object studied. It gives the initial state from which the deformation process begins.

It is well-known that the quality of deformable model-based segmentation depends significantly on the accuracy of an *a priori* model. If an *a priori* model is far from the actual location and shape, the deformation process cannot find the optimal solution because of the presence of disturbing attractors in the images. Therefore, it is important that an *a priori* model resembles the target data as much as possible. It is known that, for example, the brain images of healthy people are in many ways similar. This prior knowledge can be used to generate an *a priori* model that is close to the optimal solution. Although the imaging data of healthy people closely resemble each other, there exist also many kinds of variations. The next step in the development of better deformable model-based segmentation methods is to model these variations and utilize this prior knowledge in segmentation. This knowledge can be used to constrain the deformation process so that the results are always valid examples of the object studied. For example, in the segmentation of human brain, the deformation of an *a priori* model is allowed to generate only shapes that represent a human brain.

As mentioned above, the diagnoses are traditionally based on a physician's education and experience. The problem is that such diagnoses are subjective. Especially, if the difference between healthy and diseased individuals is small and vague, the differences in experience, routines, and even in the mood of physicians may cause divergence in diagnoses. In some cases, the differences between healthy and diseased individuals are so small that even an experienced physician cannot detect them. After the image has been segmented, quantitative information can be determined from the segmentation. In order to efficiently utilize this information in diagnoses, one has to know which quantitative values are typical to healthy people and which values are an indication of a disease. In other words, it has to be defined where the border between healthy and diseased individuals runs.

Computational methods enable objective determination of the differences between healthy and diseased individuals. For example, the stroke volumes of the heart ventricles could be measured from a big enough set of healthy individuals and from a patient to be diagnosed. By studying the variability of the volumes, one could determine how probable it is that the heart ventricles of a healthy individual have the stroke volumes determined for the patient. If this probability is smaller than a threshold, the patient is diagnosed to be diseased. Similarly, the normality of other characteristic, such as shape or function, can be determined by comparing the data of a patient to the variability in a group of healthy individuals. In other words, the modeling of the characteristics of objects is needed in computational diagnosis. Exactly the same was needed in deformable model-based segmentation methods to maximally utilize prior knowledge on the object of interest.

In the work described in this Thesis, the objective was to develop and study methods to model the shape and appearance of anatomical structures, and the variation in the shape of structures. These models were then used in deformable model-based image segmentation to produce an accurate *a priori* model and to constrain the deformation process. Also, methods that can give diagnostic information on the size and shape variations between individuals were studied.

In the future, development of the methods studied in this Thesis may give an important contribution to physicians' diagnosis making. In computer-assisted diagnosis, an automatic image analysis program retrieves the information needed from imaging data, such as the volume of object or assessment on the normality of object. The physician can then utilize this information to justify his or her diagnosis.

1.2   Outline of the Thesis

Methods to generate an accurate *a priori* model for deformable model-based methods are presented in Section 2. The modeling of the variations in the imaging data of a group of individuals and applications in deformable model-based methods are discussed in Section 3. The methods presented were applied to several applications. In Section 4, the results from deformable model-based applications are presented. The variability of shape and volume of the striatum in healthy people was studied. The methods used in the analysis and the results are presented in Section 5. The methods studied and the results obtained are discussed in Section 6. The conclusions are drawn in Section 7.

2   Methods to generate an accurate *a priori* model

The quality of segmentation depends significantly on the accuracy of an *a priori* model. The main reason for the need for the accurate initialization is the presence of disturbing attractors in the images. As an *a priori* model is deformed, it may attract to the boundaries of nearby objects. Therefore, an *a priori* model deformed to fit to the target data has to be as close as possible to the optimal solution. When a good *a priori* model exists, only small deformations are needed and the process is affected neither by the noise nor by other features in the target data.

There are several ways to generate an *a priori* model for deformable model-based segmentation methods. One can take any smooth surface, such as a sphere, and use it as an *a priori* model. Naturally, this gives a rather inaccurate initial approximation in most applications. Generally, a better approach is to randomly take one database model and use it as an *a priori* model. This guarantees that an *a priori* model has an approximately correct shape and will usually result in relatively good segmentation.

Two methods to generate an *a priori* model using information from a group of individuals were studied. In the model selection procedure (Section 2.1), the subject whose data were the most similar to the target data was searched from the database. This was done separately for each target subject. The other approach studied was to construct a mean shape or appearance model from the database (Section 2.2). The mean model is usually close to the optimal solution, and gives an accurate segmentation. A method closely related to the mean models is the combination of the results of several segmentations. Whereas in the mean models the averaging is done before segmentation, in this technique, the averaging of the data of database subjects is done after it (Section 2.3).

2.1   Model selection

The basic idea behind the model selection procedure is to select from a database the one subject whose data give the most accurate segmentation or registration when used as an *a priori* model. In registration, the data from several imaging examinations are brought to the same coordinate system. In rigid registration, the data are translated and rotated, which is usually sufficient in registration of the data of one individual, for example, from different imaging modalities or from different time instances. More degrees of freedom are required when the data of several individuals are registered, and non-rigid registration has to be used to correct local differences among individuals. Considering the studies in this Thesis, the techniques used in non-rigid registration and deformable model-based segmentation are similar.

In practice, it is not known which database subject gives the best result (the actual segmentation or registration errors cannot be determined as the correct segmentation or registration is not available). It is assumed that the more similar the database subject and the target are the better accuracy is obtained. Therefore, the similarities between the database subjects and the target are used to select one *a priori* model from the database. If the selection is successful, an *a priori* model is close to the correct solution and the segmentation or registration will be accurate.

The basic procedure of the model selection is shown in Fig. 2. The similarity, SIM, between the target, $\mathbf{t}$, and the database subjects, $\mathbf{s}_j$, is estimated using a set of similarity features, f_i, calculated from the data available. The estimation of the similarity is obtained from a linear model

$$SIM(\mathbf{t}, \mathbf{s}_j) = \sum_i w_i f_i(\mathbf{t}, \mathbf{s}_j), \qquad (1)$$
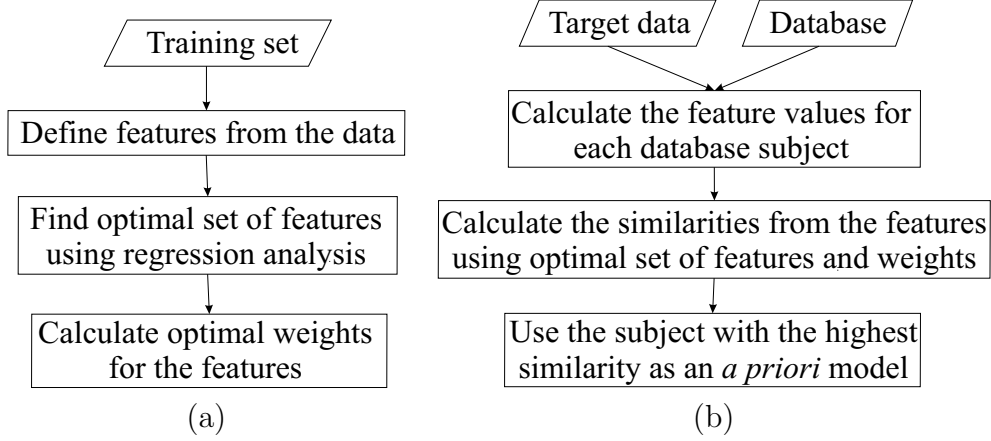
Figure 2: The procedures for (a) the training of the linear model in the model selection procedure, and (b) the application of the model selection procedure.

where w_i is the weight of the ith feature. The data of the database subject with the highest similarity value are then used as an *a priori* model.

The definition of the similarity features f_i in Eq. 1 depends on the data available. The model selection procedure was used in two applications: in segmentation of MR images (Publication VII) and in registration of an *a priori* surface model to a target point set (Publication I and VI). In the former application, measures such as the mean-squared difference in gray-level values,

$$f(\mathbf{t}, \mathbf{s}_j) = \frac{1}{N_x N_y N_z} \sum_{x=1}^{N_x} \sum_{y=1}^{N_y} \sum_{z=1}^{N_z} (\mathbf{I}_\mathbf{t}(x, y, z) - \mathbf{I}_{\mathbf{s}_j}(x, y, z))^2, \tag{2}$$

where N_x, N_y, and N_z were the dimensions of the images, were used to estimate the similarity between the gray-level image of the target, $\mathbf{I}_\mathbf{t}$, and the gray-level image of a database subject $\mathbf{I}_{\mathbf{s}_j}$. One of the best measures studied was the normalized mutual information (NMI) (Studholme et al., 1999), which measures the dependencies between the gray-level values in two images. In the latter application, the features described the similarity of the database and target shapes. One such feature was the mean distance from the target points, t_i, to the database surface, $\mathbf{s}_j$:

$$f(\mathbf{t}, \mathbf{s}_j) = \frac{1}{N_p} \sum_{i=1}^{N_p} D(\mathbf{s}_j, t_i), \tag{3}$$

where N_p was the number of the points in the target surface and $D(\mathbf{s}_j, t_i)$ the distance from the ith target point to the database surface.

The optimal set of features (to avoid over-learning of the linear model), and the optimal weights, w_i, were determined from the database using regression analysis. In segmentation and registration, the objective is to obtain as small error as possible. Therefore, the estimate of the complement of the segmentation error between the manual and automatic segmentations was used as the similarity value SIM in Eq. 1. The segmentation error (target registration error, TRE) was determined as (analogous to Fitzpatrick et al. (1998)):

$$\text{TRE} \equiv \frac{1}{N_t} \sum_{i=1}^{N_t} D(\mathbf{r}, t_i), \tag{4}$$

where N_t was the number of the points in the target surface, t_i the ith target surface point, and $D(\mathbf{r}, t_i)$ the distance from the ith target surface point to the result surface of automatic

segmentation **r**. The target surface was generated by manually segmenting the object of interest from the target data, and the surface was represented using a triangle mesh. The surface points were the nodes of the triangular surface.

The model selection can be performed both before and after segmentation or non-rigid registration. If the selection is done before, the segmentation or registration has to be done only once using the data of the database subject selected. Therefore, computation time is not increased considerably as compared to the segmentation or registration using random selection of an *a priori* model. When the selection is done after the segmentation or registration, a set of segmentations or registrations has to be made using the data of each database subject as an *a priori* model. Consequently, computation time may increase significantly. This may be an important limitation if the database is large.

The model selection procedure has been studied by Rohlfing et al. (2004a), too. They performed the selection in the same way as presented above, but used only one feature (NMI). Brejl and Sonka (2000) segmented an image using a set of shapes, and the shape that gave the best fit to the image was selected. Stegmann and Larsen (2003) constructed five different clusters of image appearance in the segmentation of perfusion MR images. The clusters represented different phases of perfusion imaging, and a statistical appearance model was constructed for each cluster. Each model was used in the segmentation of the target, and the one that gave the best fit was selected.

Marsland et al. (2003) selected the best reference subject from the database for the construction of a mean model. The selection was done based on the deformations from the reference subject to the database subjects so that the selected subject was the nearest one to the mean of the database. Gering (2003) searched for the database subject most similar to the target in local neighborhood in different resolutions using the root-mean-squared error of the gray-level values. Based on the distances to the most similar healthy database subject in different resolutions, Gering (2003) determined the probability of a pathology in the particular location.

2.2   Mean models

The models that represent the mean shape or appearance of a population can be constructed from the database. As they represent the mean of the database, they are in most cases closer to the optimal result than a randomly selected database model. Therefore, better registration or segmentation accuracy is achieved using the mean model as an *a priori* model (Publications I, VI, and VII, Lorenzo-Valdés et al. (2002); Rohlfing et al. (2004a)).

The overall procedures used for the construction of the mean shape and appearance models are represented in Fig. 3 (Guimond et al., 2000; Frangi et al., 2002; Rueckert et al., 2003). The basic idea in these procedures is to first align and then register the database subjects so that the correspondence between the subjects is obtained (spatial normalization of data or normalization of shape parametrization). For example, if the shapes are represented using a point set, the correspondence between the surface points is determined. If a mean appearance model is constructed, the transformations from the reference subject to the database subjects, $\mathbf{T}_i : \mathbf{x}_{ref} \mapsto \mathbf{x}_i$, are obtained, and these establish the spatial correspondence. Once the correspondence has been determined, the mean shape, $\bar{\mathbf{x}}$, is obtained by averaging the shape representations of the database subjects, $\mathbf{x}_i$:

$$\bar{\mathbf{x}} = \frac{1}{N} \sum_{i=1}^{N} \mathbf{x}_i. \tag{5}$$

Possible shape parametrizations include point sets (Cootes et al., 1995; Neumann and Lorenz, 1998; Fleute and Lavallée, 1998), Fourier descriptors (Staib and Duncan, 1992, 1996; Székely
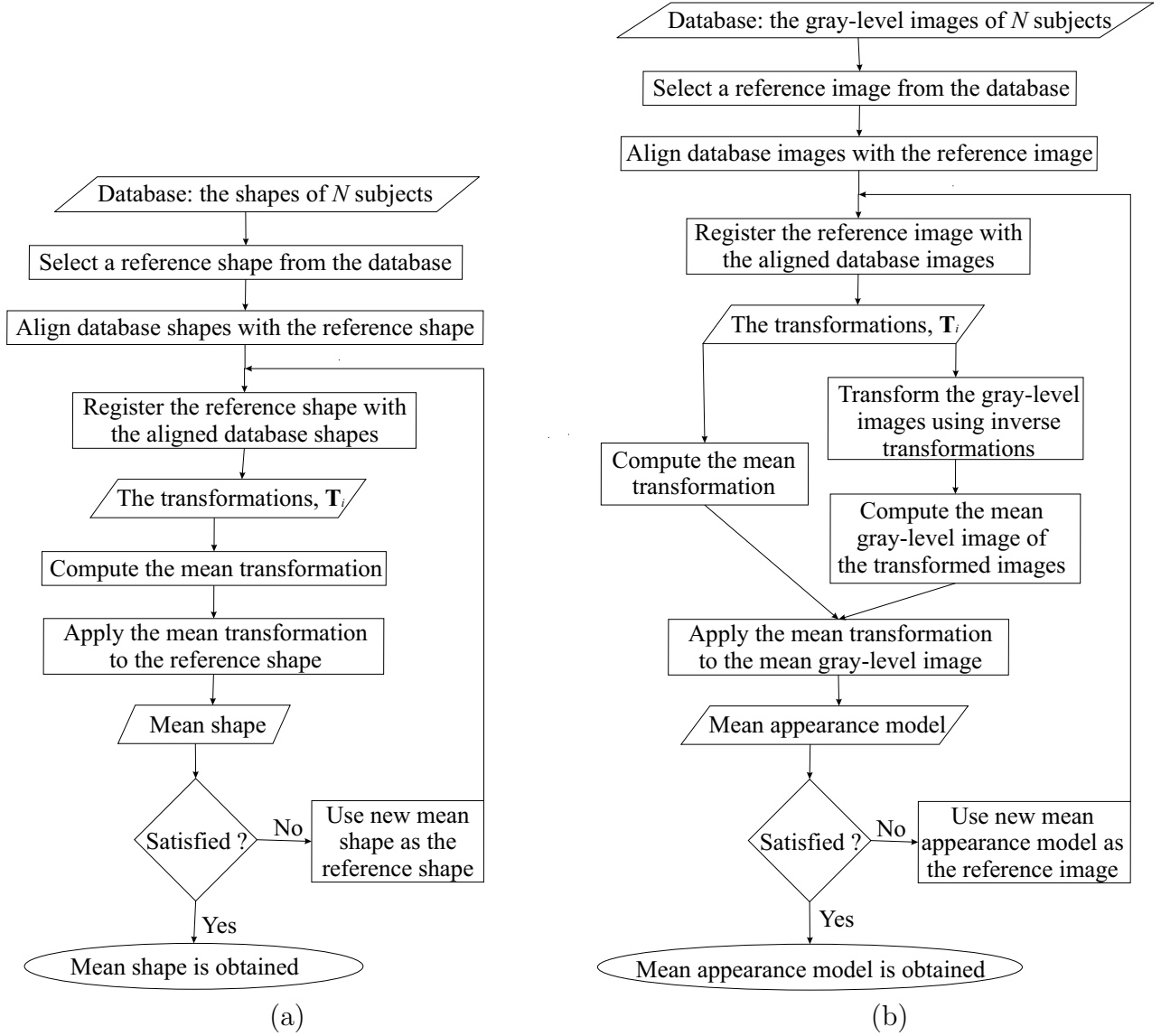
Figure 3: The procedures for the construction of the mean (a) shape and (b) appearance models.

et al., 1996; Neumann and Lorenz, 1998), spherical harmonics (Kelemen et al., 1999; van't Ent et al., 2001), splines (Baumberg and Hogg, 1995), and wavelets (Neumann and Lorenz, 1998; Davatzikos et al., 2003). The mean appearance model is constructed by first generating the mean gray-level image, $\bar{\mathbf{I}}_0$, from the spatially normalized database images, $\mathbf{I}_i$:

$$\bar{\mathbf{I}}_0 = \frac{1}{N} \sum_{i=1}^{N} \mathbf{T}_i^{-1} \mathbf{I}_i. \tag{6}$$

This image is then transformed to the coordinate system that represents the mean of the database:

$$\bar{\mathbf{T}} = \frac{1}{N} \sum_{i=1}^{N} \mathbf{T}_i, \tag{7}$$

$$\bar{\mathbf{I}} = \bar{\mathbf{T}}\bar{\mathbf{I}}_0. \tag{8}$$

Similar methods can be used to construct mean motion models as well (Rao et al., 2003). When the temporal dimension is included in the model, the correspondence has to be found both in the spatial and temporal coordinates.

The most important step in the construction of the mean models is the registration of the data to establish the correspondence between the database subjects. If the accuracy of the registration is poor, details may not be visible in the mean model, as shown in Fig. 4.

(a)

(b)
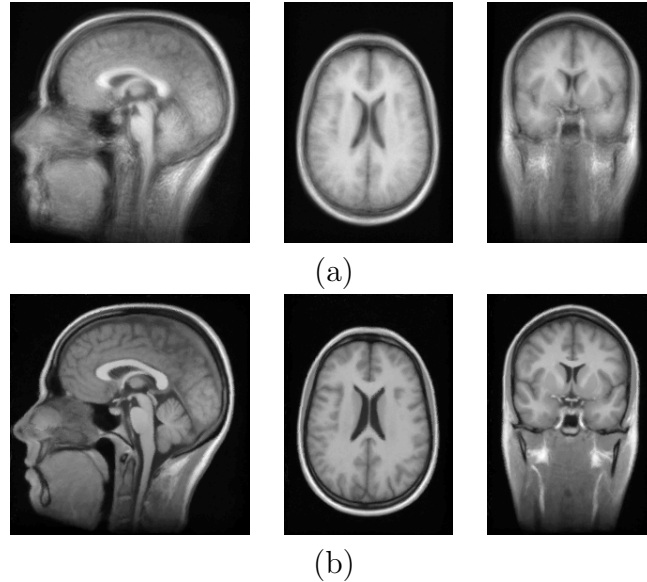
Figure 4: The effect of registration accuracy on mean appearance models. (a) A mean model using only affine registration (translation, rotation, and scaling) and (b) a mean model using non-rigid registration ($N = 31$). The models have been constructed using the procedure shown in Fig. 3b.

In practice, the choice of the reference subject affects the results: the mean model is biased towards the reference subject (Rueckert et al., 2003). Several solutions have been proposed to ease this problem. Marsland et al. (2003) used the database subject that minimized the pair-wise distance to the remaining database subjects as the reference subject. The whole procedure described above can be performed iteratively by replacing the reference subject with the mean model of the previous iteration, as shown in Fig. 3 (Publications II and IV, Cootes et al. (1995); Subsol et al. (1998); Fleute and Lavallée (1998); Guimond et al. (2000); Rohlfing et al. (2001); Frangi et al. (2002)). This reduces the bias towards the selected reference subject, and different initial reference subjects produce almost identical mean models (Subsol et al., 1998; Guimond et al., 2000; Frangi et al., 2002). In addition, by replacing the reference model with the mean model, the initial guess will likely be closer to the target in non-rigid registration, which results in more accurate registrations. In the procedure presented above, the database subjects are registered with the reference subject one at a time. However, it has been proposed that better overall registration accuracy is achieved by registering all the database subjects simultaneously (Marsland et al., 2003; Studholme, 2003; Bhatia et al., 2004; Joshi et al., 2004). Instead of finding the correspondence between the reference and all the database subjects, pair-wise correspondence and a binary tree can be used (Brett and Taylor, 2000; Hill et al., 2000).

If the mean surface model is to be constructed, one can use also methods different from the one presented in Fig. 3a. Frangi et al. (2002) constructed a mean shape model using a procedure called *shape-based blending*. In this method, the aligned signed distance maps of the database shapes were averaged, and the mean shape was obtained by thresholding the mean distance map to its zero-level. Leventon et al. (2000) and Yang and Duncan (2003) used similar level-set-based approaches. In these methods, non-rigid registration is not needed, but

the topology of the mean model may be erroneous, especially if the initial alignment is not accurate (Frangi et al., 2002).

2.3   Combination of classifiers

In the construction of mean models, the data of the database subjects are averaged before registration or segmentation. However, the averaging can be done also afterwards. The idea is that several classifications are obtained with different *a priori* models, algorithms, or parameters, and these results are combined to provide on average a more accurate classification. In practice, the registration or segmentation is usually performed using all the database models as an *a priori* model and the results obtained are combined. Naturally, this increases the computation time as the registration or segmentation has to be done for each database subject. Therefore, the computation time may become a problem if the registration or segmentation method used is time-consuming.

Segmentation defines for each voxel a label which gives the estimated class of that particular voxel. The simplest way to utilize the combination of classifiers is to select the label that gets the most votes when each database model is used as an *a priori* model (Rohlfing et al., 2004a). Rohlfing et al. (2004a) found this approach the best of the methods studied (random selection of an *a priori* model, model selection, mean models, and combination of classifiers). A generalization of this is to give a weight to each classifier (i.e., database model), which describes the reliability of the particular classifier (Warfield et al., 2002; Rohlfing et al., 2004b). In these studies, better results were reported than for the simple voting rule.

The combination of classifiers was evaluated in Publication I. The geometrical models that were obtained using all the database subjects as an *a priori* model were averaged after non-rigid registration.

3   Methods to model shape variation in the database

Models of shape variation are needed to incorporate prior knowledge on the problem in deformable model-based methods and to give diagnostic information on the differences between healthy and diseased individuals. The variations in the imaging data of a group of individuals can be modeled using either probabilistic or statistical shape models. The models describe what are the typical variations in the imaging data in the group of individuals studied.

One problem in conventional deformable models is that they are not specific to the object studied. In other words, an *a priori* model can take on almost any continuous and smooth shape. This can result in implausible segmentations or registrations, especially if the data are noisy or the initialization is poor. To improve the specificity of deformable models, both probabilistic (Section 3.1) and statistical (Section 3.2) shape models were studied. The probabilistic and statistical shape models were used to constrain the deformations so that only the shapes similar to the ones in the database were accepted.

3.1   Probabilistic shape models

The basic idea in the probabilistic methods is to model the variation in the population using some probability density function. One can model both the shape parametrization and the gray-level information. After the probabilistic model has been constructed, the deformation can be constrained so that the shapes that are similar to the database shapes or the gray-level values that are similar to the database gray-level values are favored. Therefore, it is likely that the results are similar to the ones in the database.

Basically, there are two ways to utilize probabilistic methods to constrain the deformations: probability density functions (Section 3.1.1) and probabilistic atlases (Section 3.1.2).

3.1.1   Probability density functions (PDFs)

When probability density functions (PDFs) are used to model the variability in the database, the Gaussian distribution is often used as the approximation of the underlying distribution of the shape parameters or gray-level data (Staib and Duncan, 1992, 1996; Chen et al., 1999b). This both simplifies and speeds up the calculations. For example, the probability of a shape parameter, x_j, can be modeled as a one-dimensional (1-D) Gaussian distribution. If independency of the shape parameters is assumed (Staib and Duncan, 1992, 1996), the probability of a parametrized shape, $\mathbf{x} = [x_1, x_2, \ldots, x_n]$, is

$$P(\mathbf{x}) = \prod_{j=1}^{n} \frac{1}{\sqrt{2\pi\sigma_j^2}} exp\left(-\frac{(x_j - \mu_j)^2}{2\sigma_j^2}\right), \tag{9}$$

where μ_j is the mean of the jth shape parameter and σ_j^2 the variance of the shape parameter across the database subjects. Similarly, the histogram of the intensity variations in the database can be modeled as a 1-D Gaussian distribution (Chen et al., 1999b). When the shape is parametrized using a set of points, a natural choice to model the shape variability is to use the coordinates of the points, $\vec{x}_j$:

$$P(\vec{x}_j) = \frac{1}{\sqrt{(2\pi)^d |\Sigma_j|}} exp\left(-\frac{1}{2}(\vec{x}_j - \vec{\mu}_j)^T \Sigma_j^{-1}(\vec{x}_j - \vec{\mu}_j)\right), \tag{10}$$

where d is the dimension of the space and Σ_j a $d \times d$ covariance matrix. In order to be able to construct these probability density functions, the correspondence between the database
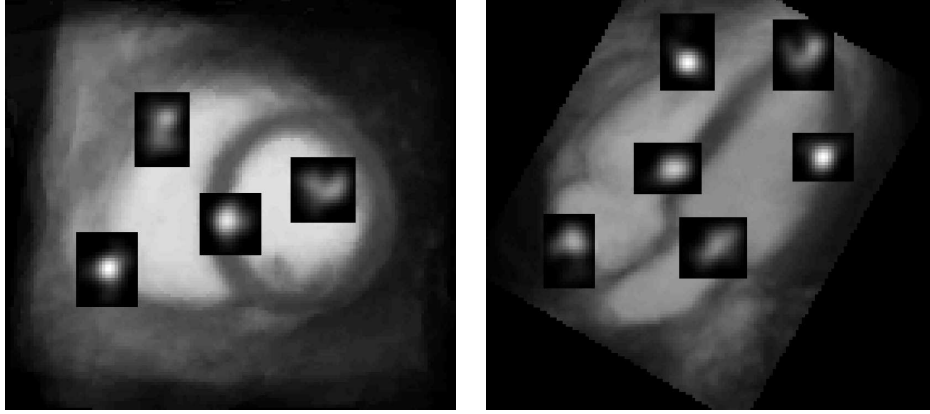
Figure 5: Non-parametric PDFs. Non-parametric PDFs of the surface points' variability for the heart ventricles and atria ($N = 25$). In each small box, the non-parametric PDF of the surface point in the center of the box is shown.

subjects has to be established. For example, if the coordinates of the model points are used, the point correspondence has to be established. If the gray-level values are modeled, the voxel-wise correspondence has to be defined.

The Gaussian distribution is not the only choice for the modeling of the database variability. For example, if the underlying distribution is curved, or has many peaks, the Gaussian distribution gives an inaccurate approximation. The non-linearities may come, for example, from the rotation of the objects, such as the twisting motion of the heart. In these cases, a more complex PDF has to be used. One possibility is to approximate the distribution using the combination of many Gaussian distributions (i.e., a mixture of Gaussians). In this Thesis, the point distributions were modeled using non-parametric PDFs with Parzen-windowing (Fig. 5) (Duda and Hart, 1973). In practice, the points were moved to the nearest voxel (i.e., nearest neighbor interpolation was used), and the counts in each voxel were calculated. The counts were normalized so that they established a real PDF. Finally, the PDF was smoothed using a Gaussian filter. The smoothing had to be done because of the small size of the database ($N = 25$).

3.1.2   Probabilistic atlases

Probabilistic atlases describe the likelihood of a shape given the database shapes. The basic idea of probabilistic atlases is the same as in the non-parametric PDFs. However, in the probabilistic atlases, only one probability map is made for the whole surface.

In the construction of the probabilistic atlases, the external variations in the data are first removed by aligning the database shapes. Usually rigid or affine registration is used, but transformations with more degrees of freedom have been used (Park et al., 2003). Next, the shapes are averaged. It can be done using the surfaces of the shapes (Fig. 6a) or the interior of the shapes (Fig. 6b). In addition, Gaussian smoothing is usually applied to the resulting atlases to guarantee smoothness. In the probabilistic atlases, the correspondence between the database shapes is not needed, which removes one major error source from the procedure. Also four-dimensional (4-D, three spatial and one temporal dimension) atlases have been constructed from the heart (Perperidis et al., 2004).
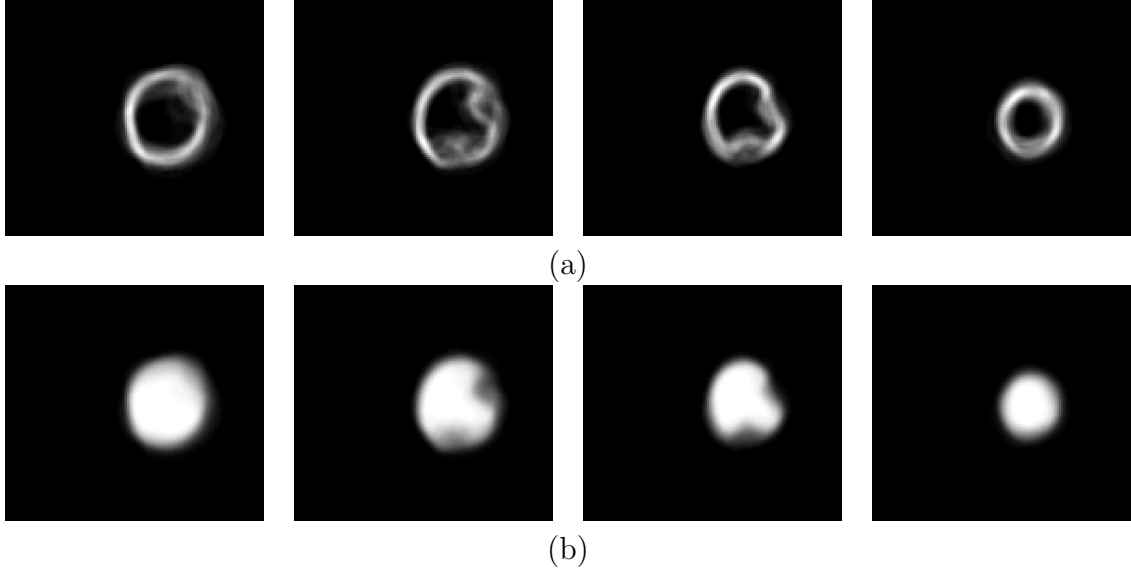
(a)

(b)

Figure 6: Probabilistic atlases. A probabilistic atlas ($N = 25$) of the left ventricle of the heart from the valve level (left) to the apical level (right): (a) using the surfaces of the shapes, and (b) using the interior of the shapes. (Publication II)

3.1.3 Applications

When the probabilistic models are used in image registration or segmentation, a natural way is to use the Bayes rule, and to maximize an *a posteriori* probability of the data (i.e., to apply the maximum *a posteriori* (MAP) criterion). The Bayes rule (see, for example, Gelman et al. (1995)) gives the relation between *a priori* probabilities of a shape, $P(\mathbf{x})$, and an image, $P(\mathbf{I})$, the likelihood of the image given the shape, $P(\mathbf{I}|\mathbf{x})$, and an *a posteriori* probability of the shape given the image, $P(\mathbf{x}|\mathbf{I})$:

$$P(\mathbf{x}|\mathbf{I}) = \frac{P(\mathbf{I}|\mathbf{x})P(\mathbf{x})}{P(\mathbf{I})}. \tag{11}$$

The likelihood term, $P(\mathbf{I}|\mathbf{x})$, describes how probable it is to achieve the image $\mathbf{I}$ when the object has the shape $\mathbf{x}$. Its objective is to match the shape to the features in the target image. The likelihood term can be determined in many ways, for example, based on image gradients, edge detectors, or voxel similarity measures. An *a priori* probability of the shape, $P(\mathbf{x})$, embeds information on typical shapes of the object, and is learned from a shape database. It biases the solution towards the shapes present in the database. An *a priori* probability of the image, $P(\mathbf{I})$, is basically only a scaling factor, and is independent of the shape $\mathbf{x}$.

In segmentation and registration, the model parameters $\mathbf{x}_{MAP}$ that maximize an *a posteriori* probability of the shape for the given image are searched. Usually, the logarithm of an *a posteriori* probability is maximized. This gives a simpler equation that can be effectively optimized:

$$P(\mathbf{x}_{MAP}|\mathbf{I}) = \max_{\mathbf{x}} P(\mathbf{x}|\mathbf{I}) = \max_{\mathbf{x}} \frac{P(\mathbf{I}|\mathbf{x})P(\mathbf{x})}{P(\mathbf{I})} \propto \max_{\mathbf{x}} P(\mathbf{I}|\mathbf{x})P(\mathbf{x}) \propto \max_{\mathbf{x}} \{\ln P(\mathbf{I}|\mathbf{x}) + \ln P(\mathbf{x})\}. \tag{12}$$

Probabilistic atlases are usually used to give *a priori* information on the location and variability of the organs, which is then used as an initialization in the segmentation (Van Leemput et al., 1999, 2001; Lorenzo-Valdés et al., 2004; Park et al., 2004). Sluimer et al. (2005) utilized a probabilistic atlas to define the border regions after the lung segmentation. In these regions, the voxels were re-classified as either object or background.

Park et al. (2003) and Sluimer et al. (2005) have reported better segmentation results for their methods with the probabilistic atlas than without it. In addition, Chen et al. (1999a) achieved improvement in their registration method by incorporating probabilistic information on the intensity and geometric variations.

3.2 Statistical shape models

In the probabilistic models (Section 3.1), the shape parameters are usually approximated to be independent to simplify the model and calculations. However, the parameters are usually inter-correlated. Therefore, the probabilistic models can take on shapes that are not present in the database and are not valid examples of the object studied. In statistical shape models, a compact representation of the shape variation, in which the shape parameters are uncorrelated, is learned from the database. Because the parameters are uncorrelated, simple constraints can be used to guarantee that the shapes generated are valid examples of the object.

3.2.1 Point distribution model (PDM)

The point distribution model (PDM) was introduced by Cootes et al. (1995). Similar procedures are used in other statistical shape models as well. The construction of a PDM consists of three steps. 1) The database shapes are represented using point sets for which the point correspondence exists. 2) The point sets are aligned in the same coordinate system. 3) The variations in the database are modeled by applying the principal component analysis (PCA) to the point sets.

It is important that the point correspondence is accurate so that the real shape variation is modeled. Cootes et al. (1995) located manually the landmarks on each database shape, and additional points were sampled equidistantly along contours. The manually located landmarks represent salient features that can be accurately located from the database images (e.g., sharp corners and points of high curvature). In most cases, especially in 3-D, manual methods are too time-consuming as the number of points required to represent the shape with an appropriate accuracy and the required database size to model all possible variations are large. Also, intra- and inter-observer errors are likely to arise in 3-D applications. Non-rigid registration can be used to automatically propagate the landmarks of the reference subject to the database subjects. Both volumetric (Publication II, Fleute and Lavallée (1998); Frangi et al. (2002); Wörz and Rohr (2003)) and surface-based methods have been proposed (Caunce and Taylor, 1999; Lorenz and Krahnstöver, 2000; Brett and Taylor, 2000; Kaus et al., 2003a). Matching of geometric features, such as the surface curvature, were used in (Tagare et al., 1995; Wang and Staib, 2000a; Shen et al., 2001; Meier and Fisher, 2002). In addition, the problem can be formulated as an explicit optimization problem (Kotcheff and Taylor, 1998; Davies et al., 2002; Thodberg, 2003).

Perhaps the most popular approach to align the landmarks is the Procrustes analysis, where the optimal least-squares fit of the corresponding point sets is searched using rigid or affine transformation (Gower, 1975; Goodall, 1991). Any other alignment method can be used, too. For example, voxel-based registration (Publication II), landmark-based registration (Székely et al., 1996; Kelemen et al., 1999; van't Ent et al., 2001), and Hough transform (Mitchell et al., 2001) have been proposed.

The shape vector consists of the concatenated landmark coordinates, $\mathbf{x} = [x_1, y_1, z_1, x_2, y_2, z_2 \ldots, x_m, y_m, z_m]$, where m is the number of landmarks. The number of the shape parameters is $n = d \cdot m$, where d is the dimension of the space. The database shapes form a cloud in an n-dimensional parameter space. The aim of the PDM is to model

the inter-subject variability in the parameter space by taking into account the dependencies between the shape parameters. The distribution of the cloud is assumed to be an ellipsoid. The mean shape (Eq. 5) gives the center of the shape cloud. The principal axes of the ellipsoid are computed using PCA. In practice, the eigenvectors and eigenvalues of the covariance matrix

$$\mathbf{\Sigma} = \frac{1}{N-1} \sum_{i=1}^{N} (\mathbf{x}_i - \bar{\mathbf{x}}) (\mathbf{x}_i - \bar{\mathbf{x}})^T \tag{13}$$

are calculated. As the database consists of N example shapes, and the size of the parameter vector is n, the database shapes span a $\min(N-1, n)$-dimensional sub-space in the parameter space, and there are $\min(N-1, n)$ non-zero eigenvectors. Each principal axis (i.e., eigenvector of $\mathbf{\Sigma}$), ϕ_i, gives a representation how the shapes in the database vary. These axes are called *the modes of shape variation*. An eigenvalue λ_i gives the amount of the variance in the database shapes that the corresponding eigenvector explains: the eigenvector with the largest eigenvalue corresponds to the longest axis of the ellipsoid and the most significant variations in the database.

New shapes that are similar to the database shapes are obtained from

$$\mathbf{x} = \bar{\mathbf{x}} + \mathbf{\Phi}\mathbf{b}, \tag{14}$$

where $\mathbf{\Phi} = [\phi_1, \dots, \phi_t]$ is a matrix consisting of the modes of shape variation, $\mathbf{b} = [b_1, \dots, b_t]^T$ a weight vector, and t the number of the modes in the model ($t \leq \min(N-1, n)$) (Fig. 7). Appropriate limits for the weights are usually determined based on the statistics of the database. Most often the weights are constrained to the values $-a\sqrt{\lambda_i} \leq b_i \leq +a\sqrt{\lambda_i}$. Typical values for a range from 2 to 3.5, which correspond to 95.45% and 99.95% of the variation in the database, respectively.

As a result, PDM gives a new, compact representation of the shape (i.e., the weights $\mathbf{b}$) in a new, uncorrelated basis defined by the modes of shape variation. The number of the weights, t, is usually much smaller than the number of the original shape parameters.

3.2.2   Statistical deformation model (SDM)

In PDM, the point sets or surfaces are modeled. Statistical deformation model (SDM) (Rueckert et al., 2003) is a closely related method, in which voxel-wise comparison is done using deformation fields. This enables the modeling of the whole image and all the objects in it. Using SDMs, for example, voxel-based registration can be performed.

In SDMs, non-rigid registration is used to establish the voxel-wise correspondence between the database subjects. For each voxel, a deformation vector $\mathbf{d}(x, y, z)$ is obtained, which defines the displacement of the voxel. Consequently, the deformations produce dense sets of points, so-called pseudo-landmarks, for which the correspondence exists. Rueckert et al. (2003) used free-form deformation (FFD) to establish the correspondence between the database subjects. In FFD (Sederberg and Parry, 1986; Rueckert et al., 1999; Lötjönen et al., 1999), a regular grid of control points is used to parametrize the deformation:

$$\mathbf{d}(x, y, z) = \sum_{i=0}^{l} \sum_{j=0}^{m} \sum_{k=0}^{n} Q_{l,i}(x) Q_{m,j}(y) Q_{n,k}(z) \mathbf{P}_{ijk}, \tag{15}$$

where $Q_{l,i}$ is a polynomial basis function (e.g, linear basis function or B-spline), and $\mathbf{P}_{ijk}$ are the positions of the grid points. FFD produces a smooth and continuous deformation.

As the FFD grid points' coordinates parametrize the deformation, a compact representation of the deformations is achieved by keeping only the displacements of the control points. In SDM,

First mode

Second mode

Third mode

Fourth mode

$$\bar{\mathbf{x}} - 3 \cdot \sqrt{\lambda_i}\phi_i \qquad\qquad \bar{\mathbf{x}} \qquad\qquad \bar{\mathbf{x}} + 3 \cdot \sqrt{\lambda_i}\phi_i$$
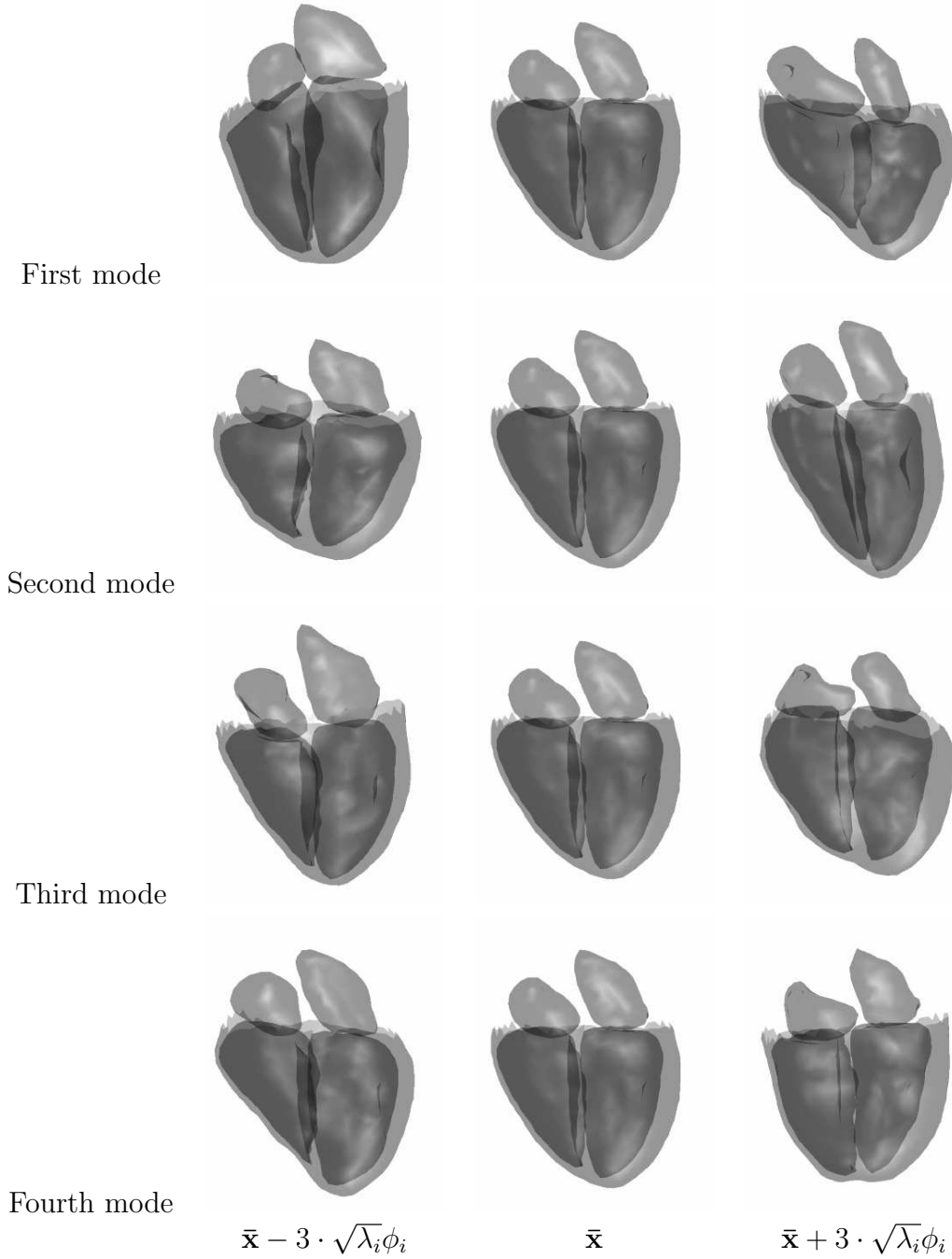
Figure 7: Statistical shape model. New shapes are obtained by varying the weights of the modes of shape variation. (Publication II)

PCA is applied to the variations in the grid points' coordinates. New, valid examples of the shape can be generated by applying the deformation $\mathbf{d}$ obtained with the linear model

$$\mathbf{d} = \bar{\mathbf{d}} + \mathbf{\Phi}\mathbf{b}, \tag{16}$$

where $\bar{\mathbf{d}}$ is the mean deformation, $\mathbf{\Phi}$ contains the eigenvectors (so-called *statistical deformation modes*), and $\mathbf{b}$ is a weight vector, to the reference shape.

In addition to the surface points and the FFD grid, statistical shape models can be constructed from other shape representations, too. The methods proposed in the literature include orthogonal basis functions, such as Fourier descriptors (Staib and Duncan, 1992, 1996; Székely

et al., 1996), cubic B-splines (Baumberg and Hogg, 1995), wavelets (Neumann and Lorenz, 1998; Davatzikos et al., 2003), and spherical harmonic functions (Kelemen et al., 1999; van't Ent et al., 2001), medial representation (Pizer et al., 1999; Golland et al., 1999; Joshi et al., 2002; Styner et al., 2003), and level-set functions (Leventon et al., 2000; Tsai et al., 2003; Yang et al., 2003, 2004).

3.2.3   Enlargement of the database

The number of model parameters, n, is usually so large that the number of non-zero eigenvalues is determined by the number of database subjects, N (i.e., the number of modes of shape variation is $N-1$). The required size of the database increases notably in 3-D as compared to 2-D (Kelemen et al., 1999; Ordas et al., 2004). Today in many of the studies with the statistical shape models, the databases are too small (under 50 subjects). For example, Frangi et al. (2002) constructed a 3-D statistical shape model of the cardiac ventricles from the short-axis MR images of 14 healthy adults, Rueckert et al. (2003) constructed a 3-D statistical brain model from 25 MR images of subjects with schizophrenia, Kelemen et al. (1999) used 22 subjects in their hippocampus model, and Chandrashekara et al. (2003) built a 3-D+time statistical motion model of the heart from the tagged MR images of 17 subjects. The anatomical variability of many objects is so large that it cannot be accurately modeled with so few modes of shape variation. Consequently, the model restricts the shape too much and the segmentation accuracy is limited.

It is often very laborious to expand the database as many of the methods require manual segmentations of the objects of interest and the registration of the data may take a long time. Also, the imaging data needed are not always available. If there are no real data available or they cannot be used, one option is to increase the smoothness, and, therefore, the generality of the model, artificially. Smooth variations can be generated using physical models (Sclaroff and Isidoro, 1998). This provides a model allowing variability due to the physical model and specificity due to the information on the database variations. Cootes and Taylor (1995) constructed a synthetic covariance matrix which included both real shape variation from the database and synthetic, physical shape variation. Wang and Staib (2000a) made a synthetic covariance matrix which incorporated smoothness constraints. This was then combined with the covariance matrix generated from the database using weighted averaging. Baumberg and Hogg (1995) added noise to the covariance matrix to enable the generation of new shapes which have small details that are not present in the database. Another option is to generate more example shapes using the existing database. As the number of the shapes in the database increases, more modes of shape variation can be constructed from the data, and the model is less constrained. Davatzikos et al. (2003) proposed two hierarchical approaches. In the first one, the shape was partitioned into smaller segments. Statistical models were constructed separately for each segment and for the mass centers of the segments. The second approach used wavelets to decompose the shape into a set of bands, and the modes were calculated separately for each band.

In Publication V, several methods were studied to artificially enlarge the database. In addition to the basic PCA model, six methods were tested. As the best one emerged the non-rigid movement technique, in which new shapes were generated by deforming the real database shapes randomly, locally, and non-rigidly. A sphere (radius r) was located in the shapes, and the center point (c_x, c_y, c_z) was translated using a random vector $\mathbf{V}$. The points inside the sphere were displaced using the equation

$$\mathbf{v}(x, y, z) = \frac{e^{-2\frac{(x-c_x)^2+(y-c_y)^2+(z-c_z)^2}{r^2}} - e^{-2}}{1.0 - e^{-2}}\mathbf{V}. \tag{17}$$

3.2.4   Applications

The goal in the statistical shape model-based image segmentation and registration is to find such values for the model parameters (**b** in Eq. 14) that the model fits the target data as closely as possible. Active shape models (ASMs) were presented by Cootes et al. (1995) to perform the segmentation with a PDM. In ASMs, the gray-scale profiles perpendicular to the surface in each landmark are used to iteratively establish an optimal deformation, while constraining the shape based on the PDM (Cootes et al., 1995; Duta and Sonka, 1998; Kelemen et al., 1999; Cootes and Taylor, 2004; Brejl and Sonka, 2000; van Ginneken et al., 2002). The optimization can be done using other kinds of objective functions, too. In SDM, a natural choice is to use an intensity similarity measure (Publication II, Loeckx et al. (2003)). A curve was matched to an edge map in (Székely et al., 1996). When incomplete data are used, the mean distance between target data points and surface model is minimized (Publications I and VI, Fleute and Lavallée (1998); van't Ent et al. (2001)). The MAP framework can also be used in the statistical model-based segmentation or registration. Usually a Gaussian distribution is assumed for the shape parameters (Leventon et al., 2000; Wang and Staib, 2000b). In addition, statistical shape information can be used in a regularization term (Kaus et al., 2003b). The robustness, speed, and accuracy of the statistical model-based methods can be improved by using hierarchical or multi-resolution implementation (Cootes et al., 1994; Székely et al., 1996; Shen et al., 2001; van Ginneken et al., 2002; Davatzikos et al., 2003).

4   Studied methods applied to segmentation and registration

The methods presented to model prior knowledge and utilize it in deformable model-based methods were studied, evaluated, and compared in different applications. These applications and results obtained are presented in this section.

4.1   Model selection in segmentation of MR images

The performance of the model selection in segmentation of MR images was evaluated by studying how well the method succeeded in selecting a database model similar to the target data (Publication VII). The method was compared to the random selection of an *a priori* model. In practice, the random selection was evaluated by using the data of each database subject as an *a priori* model and averaging the segmentation errors. This study, like all studies in this Thesis, was done using leave-one-out cross-validation. In other words, each subject was once removed from the database and regarded as a target. The remaining subjects established the database used for the particular target subject.

The database consisted of nine subjects and the method was evaluated for five structures (skin, brain envelope, cerebellum, corpus callosum, and midbrain). The model selection procedure improved the segmentation accuracy as compared to the random selection of an *a priori* model. For the intensity-based segmentation of the brain structures, the model selection procedure gave better accuracy than the random selection in 97.8% of the cases, as averaged over all the target subjects and all the objects. The best model was selected in 48.8% of the cases (if random selection had been used, this figure would have been 12.5%). The model selection procedure gave 78.6% improvement from the random selection as compared to the maximum possible (the improvement would have been 100% if the best model had always been selected). Similar results were obtained also for the surface-based segmentation tested. For each brain structure and segmentation method studied, the segmentation accuracy was statistically significantly better when the model selection procedure was used as compared to the random selection of an *a priori* model (Wilcoxon signed rank test, $p = 0.05$).

4.2   3-D geometry from incomplete data

Methods to construct 3-D geometric models of head (Publication I) and thorax (Publication VI) from incomplete data were studied. A set of points was digitized from the surface of skin and an *a priori* geometric model was registered to these data. An alternative way to construct these models is to segment the objects of interest from an MR image of a subject. This provides good accuracy but MR imaging is expensive and time-consuming. The methods studied enable a fast and low-cost construction of geometric models for the applications where the accuracy of the geometric model needed is moderate.

The model selection, mean models, combination of classifiers, and statistical shape models were evaluated. The basic idea was to match an *a priori* geometric model, a triangular surface model, to the points digitized from the surface of the skin of the target subject. The databases consisted of the MR images of 15 subjects in the head study and of the MR images of 22 subjects in the thorax study. The objects of interest, (skin, scalp, and brain in the head study, and torso, lungs, and heart in the thorax study) were segmented manually from the MR images. In addition, a set of points was located manually from the MR images to simulate the digitizing of the points from the skin.

Table 1: The results (mean TRE, mm) for the construction of geometric models from incomplete data. The results for the head study are presented for three point sets. (Publications I and VI)

	Random selection	Model selection, before	Model selection, after	Model selection, separate	Mean model	Combination of classifiers	SDM
Head (PS1)	2.76	2.32	2.53		2.25	2.08	2.38
Head (PS2)	2.54	2.11	2.14		2.02	1.94	2.22
Head (PS3)	2.11	1.82	1.77		1.72	1.68	2.00
Thorax	11.23	9.19		8.93	8.80		9.10

Point set PS1 consisted of 22 points, PS2 of 44 points, and PS3 of 1155 points. In the thorax study, 23 points were used.

Columns from the left: random selection of an *a priori* model, model selection before non-rigid registration, model selection after non-rigid registration, model selection before non-rigid registration with separate selections for the torso and internal organs, registration using mean surface model, combination of classifiers, and registration using SDM.

In model selection, the database model that was estimated to be the best for the target was registered with the point set using FFD. Additionally, mean model was used as an *a priori* model, too. In the combination of classifiers, all the database models were used as an *a priori* model, and the geometric models obtained were averaged. The registration using statistical shape models was implemented using SDM, in which the weights of SDM were optimized so that the mean distance between the target points and the model surface was minimized. Fleute and Lavallée (1998) introduced a similar method to reconstruct a complete 3-D shape from a digitized point set by optimizing the pose and PDM parameters. Also van't Ent et al. (2001) estimated the complete 3-D geometry from sparse data. In their method, the surface of the skin was represented using spherical harmonic functions. The coefficients of the spherical harmonic functions of the skull and brain surfaces were then predicted from the coefficients of the skin using a linear model trained from database shapes.

The results for the construction of 3-D geometric models from the point sets are presented in Table 1. In each case studied, the model selection procedure improved the registration accuracy as compared to the random selection of an *a priori* model. Furthermore, by performing separate model selections for the torso and the internal organs (heart and lungs), the error was further decreased. The crucial question in the model selection procedure is how reliably the similarity (i.e., the TRE) of the database subjects to the target subject can be estimated from the data available. It is likely that the better the registration of the database and the target before the model selection is the better selection can be made. Therefore, if the computation time is not an issue, in many cases the model selection should be done after all the database subjects have been used as *a priori* models in non-rigid registration or segmentation. This was found to be the best approach by Rohlfing et al. (2004a). However, the sparse information from which the model selection was done in Publication I was not ideal for this purpose. The less points were used the more completely the discriminative information between the database subjects was utilized during the non-rigid registration. Consequently, for the two sparsest point sets, the model selection after the non-rigid registration gave even worse results than before it. Only with the densest point set better results were obtained by selecting the best model after the registration.

Good results were obtained in both studies using mean models and the combination of
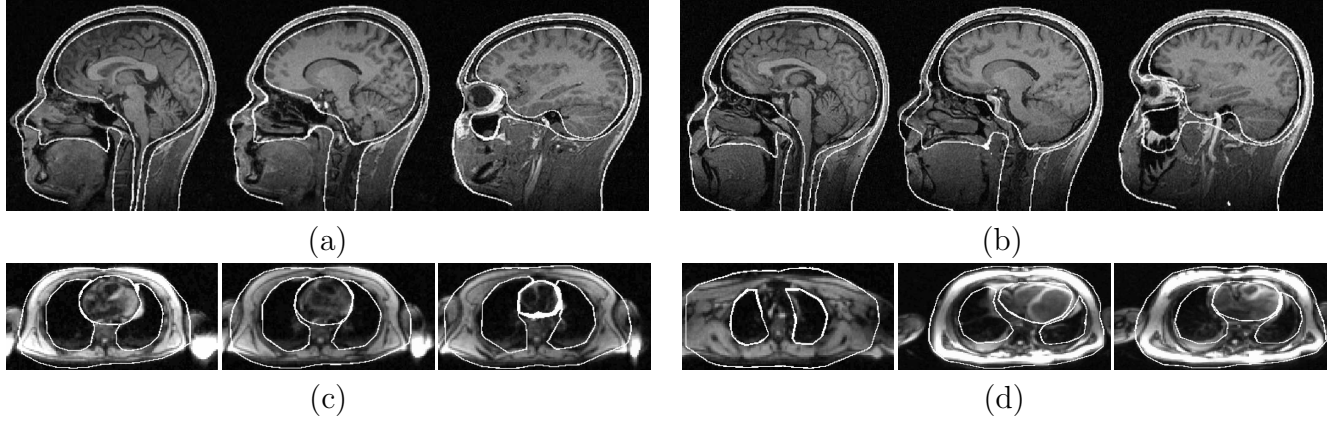
Figure 8: Example results for the construction of 3-D geometry from incomplete data. (a) The best and (b) the worst result for the sparsest point set (22 points) in Publication I for the combination of classifiers. (c) The best and (d) the worst result for the sparsest point set (23 points) in Publication VI for the model selection with the correction of internal organs.

classifiers. In the head study, these were the best methods studied, and in the thorax study, the mean models gave better accuracy than the model selection procedure. Good performance of the mean models and combination of classifiers was reported also by Rohlfing et al. (2004a).

A model that describes the correlations between the surface points' coordinates and the size and location of the internal organs was learned from the database in Publication VI. This approach, combined with the model selection, performed better than the other methods studied (mean $TRE = 7.64$ mm). Example results for the best methods of both the head and thorax studies are shown in Fig. 8.

SDMs were not able to give good results, but the other methods studied gave usually better results. For the thorax study, the accuracy of SDM was considerably better than the accuracy of the basic FFD approach with no database information. Especially, the registration accuracy of the internal organs, from which no imaging data were available, was much better using SDM. However, the mean models and the model selection procedure outperformed SDM. In the head study, the results were similar: SDM outperformed the basic FFD approach, but the combination of classifiers, mean models and model selection gave better registration accuracy.

4.3   Segmentation of cardiac structures

The segmentation of cardiac structures was performed by utilizing simultaneously both short-axis (SA) and long-axis (LA) cardiac MR images. The SA and LA images were aligned in the same coordinate system using header information and intensity-based registration (Lötjönen et al., 2005). After this, the information in SA and LA images could be compared and utilized in segmentation. The utilization of both SA and LA MR images enabled the accurate analysis of the ventricles in the basal and valve levels, and of the atria. Single image slices from different directions have been used by Lelieveldt et al. (2003) and Oost et al. (2003), but the use of volume images from different directions in segmentation of cardiac MR images is a novel idea. To author's knowledge, the statistical modeling and segmentation of atria from MR images have not been studied by any other group. Most of the recent cardiac segmentation studies using MR images have focused on the segmentation of the left ventricle and epicardium (Suri, 2000; Mitchell et al., 2002; Kaus et al., 2003a; Paragios, 2003). In some studies, also the right ventricle has been segmented (Mitchell et al., 2001; Lorenzo-Valdés et al., 2002; Gering, 2003; Lorenzo-Valdés et al., 2004; Perperidis et al., 2005). Although the LA images were used by

Lelieveldt et al. (2003) and Oost et al. (2003), only the left ventricle was segmented in these studies. Also, the atria were not included in the statistical shape models constructed by Frangi et al. (2002) and Rao et al. (2003).

In Publication IV, mean appearance models ($N = 25$) were constructed for both SA and LA images, and they were used in the deformable model-based segmentation of the four heart chambers and epicardium. It was shown, that 1) the mean models (mean $TRE = 2.99$ mm) give much better segmentation accuracy than the random selection of an *a priori* model (mean $TRE = 4.22$ mm), and 2) the use of both SA and LA images enables the accurate segmentation of atria and improves the segmentation of ventricles as compared to the segmentation using only SA images (Fig. 9).

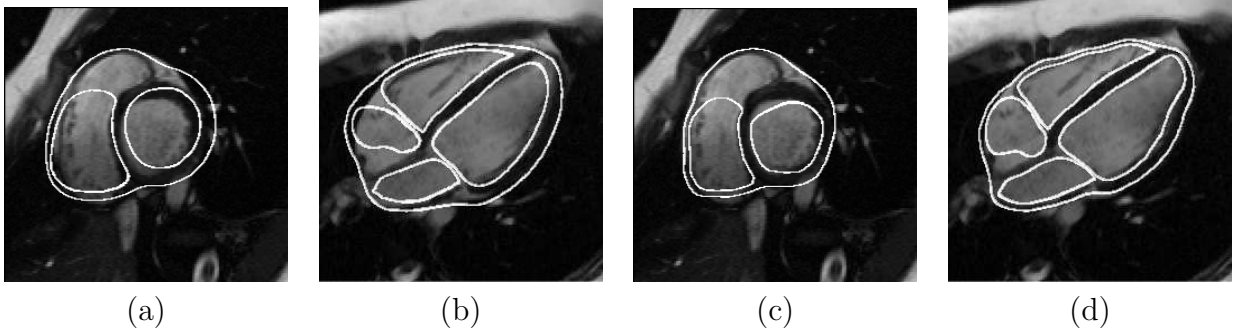| (a) | (b) | (c) | (d) |

Figure 9: Example results for the segmentation of cardiac structures. An SA and LA image slice of the segmentation results for one database subject: (a) SA and (b) LA slice after affine registration ($TRE = 3.83$ mm), and (c) SA and (d) LA slice after non-rigid registration-based segmentation ($TRE = 2.96$ mm). (Publication IV)

Statistical and probabilistic shape models of the heart were constructed from 25 healthy subjects using both SA and LA MR images in Publication II (Fig. 7). Then, these models were used to constrain the segmentation of the heart. The segmentation using statistical shape models was implemented by optimizing the weights of the SDM constructed from the database so that the NMI between the SA and LA images of the model and target was maximized. In addition to PCA, the modes of shape variation were calculated using independent component analysis (ICA) (Hyvärinen et al., 2001). It has been reported that the PCA- and ICA-based modes of shape variation have different characteristics in spatial deformations: PCA produces global deformations, while ICA produces more local modes of shape variation (Üzümcü et al., 2003; Koikkalainen and Lötjönen, 2004). Therefore, there could be differences in the segmentation performance of the methods. In the probabilistic framework, the deformations were generated using a method based on deformation spheres (Lötjönen and Mäkelä, 2001). The deformations were optimized by maximizing the energy term

$$E = E_{NMI} + \gamma E_{shape}, \tag{18}$$

where the weight γ was chosen empirically. The first energy term was the likelihood term, which was determined as the NMI between the target and model SA and LA images. The second term contained the probabilistic information on the shape variation, and it was defined as

$$E_{shape} = \frac{1}{n} \sum_{j=1}^{n} \ln P(\vec{x}_j). \tag{19}$$

Two methods were evaluated. In the first method, the probability of the surface point, $P(\vec{x}_j)$, was determined from the non-parametric PDF of the surface point (Fig. 5). In the second one, the probability of the point was determined from the probabilistic atlas of the surface (Fig. 6a).

Table 2: The errors (mean TRE, mm) for the segmentation of the heart using probabilistic and statistical shape models. (Publication II)

Method	Left ventricle	Right ventricle	Left atrium	Right atrium	Epicardium	Total
No constraints	2.32	3.87	3.83	4.38	3.61	3.60
Non-parametric PDFs	2.23	2.55	3.00	3.93	2.78	2.90
Prob. atlas	2.01	2.37	2.56	2.93	2.77	2.53
PCA-modes	2.40	2.95	3.78	4.42	3.02	3.31
ICA-modes	2.47	2.91	3.87	4.22	3.11	3.32

The results for the segmentation of ventricles, atria, and epicardium from cardiac SA and LA MR images are shown in Table. 2. All the methods studied gave better results than the unconstrained segmentation, and the statistical shape models were less accurate than the probabilistic shape models. For comparison, intra- and inter-observer variabilities of $1 - 2$ mm have been reported for manual segmentation of cardiac structures (Publication II, van Assen et al. (2005)).

4.4   Enlargement of the database

The artificial enlargement of the database (Publication V) showed that at least in theory the performance and generality of the statistical shape models can be improved. The effects of the enlargement were studied first in a 2-D application, in which it was studied how accurately the statistical shape model (PDM) can approximate known shapes. It was observed that the artificial methods gave good improvement in the approximation accuracy (point-to-point distance E). While the basic PCA with 25 modes produced an average error of $E = 2.5$ mm, the non-rigid movement technique with 200 modes gave an average error of $E = 0.3$ mm. This showed that the artificial models were more general and could approximate much more accurately unseen shapes. In a 3-D study, the non-rigid movement technique gave similar results and succeeded to decrease the approximation error.

5 Shape analysis

Shape analysis provides methods for computer-assisted diagnosis. By studying the shape variations in a group of individuals, the differences between healthy and diseased individuals can be modeled and objective diagnostic information can be provided to physicians. In this Thesis, it was studied how the shape of the striatum changes with age and what the shape differences between genders are. However, the methods presented could be used to study the effects of diseases on the shape of the striatum or other anatomical structures, as well.

The shape of brains is very difficult to analyze visually. Many diseases cause small local shape changes in brain structures. Also, the shape changes due to, for example, aging cannot be identified visually. Therefore, the normality of the individual's brains and various differences in the shape of the brain structures have to be analyzed utilizing a group of individuals. By studying the inter- and intra-group variations, conclusions on the shape changes and differences can be made. The shape analysis is often done by comparing the subjects of two groups. For example, the two groups may consist of subjects with different ages or genders (cross-sectional studies). Another possibility is to compare the brains of same individuals in different time instances (longitudinal studies). The asymmetry of the brain structures can be examined by comparing the hemispheres of an individual.

By examining the normal, healthy brains and their asymmetry, the development of the brains in childhood (Blanton et al., 2004), the effects of aging (Resnick et al., 2000; Kovalev et al., 2003; Wang et al., 2003; Liu et al., 2003), or the shape differences between the genders (Xu et al., 2000b; Kovalev et al., 2003; Blanton et al., 2004; Bouix et al., 2005) can be studied. Studies with monozygotic and dizygotic twins can reveal information on the effects of genetics and environment on the brain development (Le Goualher et al., 2000). Disease-related shape changes and asymmetries can be observed by studying the diseased individuals (Rusch et al., 2001; Wang et al., 2001; Posener et al., 2003; Wang et al., 2003; Levitt et al., 2004). The control group consisting of the healthy subjects and the study group consisting of the patients are compared, and the effects of the disease on the shape, asymmetry, and time-dependent changes of the brain structures can be discovered. This will give information on the origin and development of the diseases, and on the effects on anatomy. Utilizing siblings and twins in the analysis, the genetic factors and heritability of the diseases can be studied (Tepest et al., 2003; van Haren et al., 2004; Styner et al., 2005). Disease-specific patterns in the shape, its development, and asymmetry will enable the early detection of the diseases, which will enable the early start of the treatment (Aylward et al., 2004; Csernansky et al., 2005).

5.1 Methods

5.1.1 Volume analysis and shape indices

The simplest possibility to study objects and their variability is to analyze their volumes. For this purpose, the objects are segmented from the imaging data, the volumes are compared, and the differences between the two groups or the volume changes in the longitudinal studies are statistically analyzed. Numerous volumetric studies have been presented, where the effects of aging (Publication III, Gunning-Dixon et al. (1998); Raz et al. (2001); Gunduz et al. (2002); Liu et al. (2003); Blanton et al. (2004)), gender (Publication III, Raz et al. (2001); Blanton et al. (2004)), and diseases (Buchsbaum et al. (1997); Rusch et al. (2001); Posener et al. (2003); van Haren et al. (2004)), and the asymmetry of the brain (Publication IV, Buchsbaum et al. (1997); Rusch et al. (2001); Pujol et al. (2002); Blanton et al. (2004)) have been studied. A standard way to study the volumes of brain structures is to co-vary the volume with the whole brain volume to take into account the individual differences in overall brain size.

Volume analysis can detect large shape differences that cause relatively global atrophy, dilation or asymmetry of the structure of interest. However, the volume alone does not give a thorough description on the structure. For example, the volumes of two completely different shapes can be identical, and an important local shape variation does not necessary result in a detectable volume change. Furthermore, the normal variability in the volumes makes the analysis more difficult. Even if statistically significant volume differences could be detected, one does not know where, for example, the local atrophy occurs. Therefore, more detailed shape analysis is needed for more accurate understanding of the human brain and its changes, and to discover age-, gender-, and disease-related shape changes (Csernansky et al., 1998; Tepest et al., 2003; Posener et al., 2003; Styner et al., 2005).

A bit more detailed analysis method was presented for the caudate nucleus by Levitt et al. (2004). A global shape index which measured the sphericity was calculated for each shape, and a group comparison was performed for this index. Other global indices proposed include the cross-sectional area (Xu et al., 2000b), surface area, and depth of the object of interest (Magnin et al., 2004). The global shape indices can reveal information on the global shape differences, but they do not give information on the location of the shape differences.

5.1.2   Local shape analysis

The progress in brain atlases and high-dimensional mapping have enabled the accurate local computational analysis of the brain structures (Thompson and Toga, 2002). One can focus on the shape of one particular sub-cortical brain structure, such as the hippocampus, or the analysis can be performed on the whole brain volume. In this Thesis, the former approach is used. Detailed shape analysis of a particular brain structure can be done by utilizing the correspondence between the shape representations. The structure is segmented, and the correspondence is established. This is mostly done using high-dimensional mapping (Publication III, Christensen et al. (1997); Davatzikos (1997); Bookstein (1997); Thompson and Toga (2002); Csernansky et al. (2004)), but spherical harmonic-based correspondence (Shenton et al. (2002); Styner et al. (2004, 2005)) and medial representation (Joshi et al. (2002); Styner et al. (2003, 2004); Bouix et al. (2005)) have been used, too.

After the correspondence has been found, the shapes of the control and study groups can be compared, and the statistically significant group differences identified. The signed distances between the study shape and the template or the subject pair were utilized in (Publication III, Csernansky et al. (1998); Tepest et al. (2003); Lee et al. (2004); Styner et al. (2004, 2005); Golland et al. (2005)). One can use either the signed distances between the corresponding points (Publication III, Csernansky et al. (1998); Tepest et al. (2003); Lee et al. (2004); Styner et al. (2005)) or the signed distance maps (Styner et al. (2004); Golland et al. (2005)). By applying statistical analysis to the group differences in the distance values in each point, statistically significant local shape changes can be detected and visualized. In medial representation, the local radii of the structure (Bouix et al., 2005), the location and the thickness of the medial atoms (Styner et al., 2003, 2004), or features computed from the medial atoms (Joshi et al., 2002) can be analyzed. Narr et al. (2004) used the distance of the surface points from the medial curve to study the shape.

A discriminant function is needed if unseen shapes are classified to one of the groups studied. One option is to construct a PDM (Section 3.2.1) from the point correspondence of the surface points (Publication III, Csernansky et al. (1998); Tepest et al. (2003)). The weights for each database subject are computed from

$$\mathbf{b}_i = \mathbf{\Phi}^T(\mathbf{x}_i - \bar{\mathbf{x}}), \tag{20}$$

and the discriminant function is obtained using one weight or a linear combination of the weights. Another technique to construct a discriminant function is to use the mean shapes of the groups (Publication III). The difference between the means is calculated and represented as a vector where the x-, y-, and z-coordinates are concatenated. The deviations of the shapes from the mean of the both groups ($\mathbf{x}_i - \bar{\mathbf{x}}$) are projected to the difference vector. The norm of the projection gives a scalar value for each subject, and the discrimination can be done based on this value. The global shape difference patterns can be studied and visualized using the discriminant functions, too (Publication III, Csernansky et al. (1998); Tepest et al. (2003); Golland et al. (2005)).

In asymmetry studies, the correspondence between the hemispheres of the same subject is established (Publication III, Wang et al. (2001)), whereas in the longitudinal studies it is established between different time-instances (Wang et al., 2003). In statistical analysis, the deviations from zero are studied in both of these techniques. Otherwise, the analysis can be done using the same methods as in the normal shape analysis.

The other methods presented for the shape analysis are the voxel- (VBM) and the deformation (DBM)-based morphometry. These techniques are usually used to study the whole brain, and the analysis is not focused on any particular brain structure. In VBM (Ashburner and Friston, 2000; Resnick et al., 2000; Good et al., 2001; Watkins et al., 2001; Park et al., 2004; Barrick et al., 2005) the images are aligned into the same coordinate system, the images are segmented into white brain matter, gray brain matter, and cerebrospinal fluid (CSF), and the distributions of the classes in each voxel within and between groups are compared. In DBM, the voxel-wise correspondence is established using high-dimensional mapping, and the resulting deformation fields are used to analyze the brain differences (Thompson et al., 1997; Ashburner et al., 1998; Thirion et al., 2000; Gaser et al., 2001). The deformation fields (Thompson et al., 1997), their parameters (Ashburner et al., 1998), or features computed from the norm, divergence, and Jacobian determinant of the deformation fields (Thirion et al., 2000; Gaser et al., 2001) give information on the local shape and volume changes.

Similar methods that are used for the sub-cortical structures can be also applied to the cortex. By mapping the cortical surfaces of the individuals, the structure of the cortex and its changes can be studied (Thompson et al., 1997; Royackkers et al., 1999; Le Goualher et al., 2000; Free et al., 2001; Csernansky et al., 2004; Magnin et al., 2004; Thompson et al., 2004).

5.2   Results

Several studies have been made in which the striatum, or its components (putamen, caudate nucleus and nucleus accumbens) have been the objects of interest. In many studies, the effects of a disease on the volume of the striatum have been studied (Shihabuddin et al., 2001; Strakowski et al., 2002; Gunduz et al., 2002; Levitt et al., 2002; Lacerda et al., 2003; Buchsbaum et al., 2003; Aylward et al., 2004; Deshmukh et al., 2005; Hollander et al., 2005). In (Levitt et al., 2004), the simple shape index showed differences in the shape of the caudate nucleus between schizophrenic and healthy subjects. Medial representation was used to study shape differences in schizophrenia by Sampath et al. (2003). In addition, inferences on the shape changes of the striatum can be made from the volumetric analysis results of the VBM and DBM studies (e.g., Gaser et al. (1999); Watkins et al. (2001)). The effects of aging on the volume of the striatum have been studied by Gunning-Dixon et al. (1998), Gunduz et al. (2002), and Brabec et al. (2003).

The volume and shape of the striatum were analyzed in Publication III. Especially, the effects of aging and gender and asymmetries were studied. The striatum was manually segmented from the MR images of 43 subjects, and the volumes were determined. The same was done
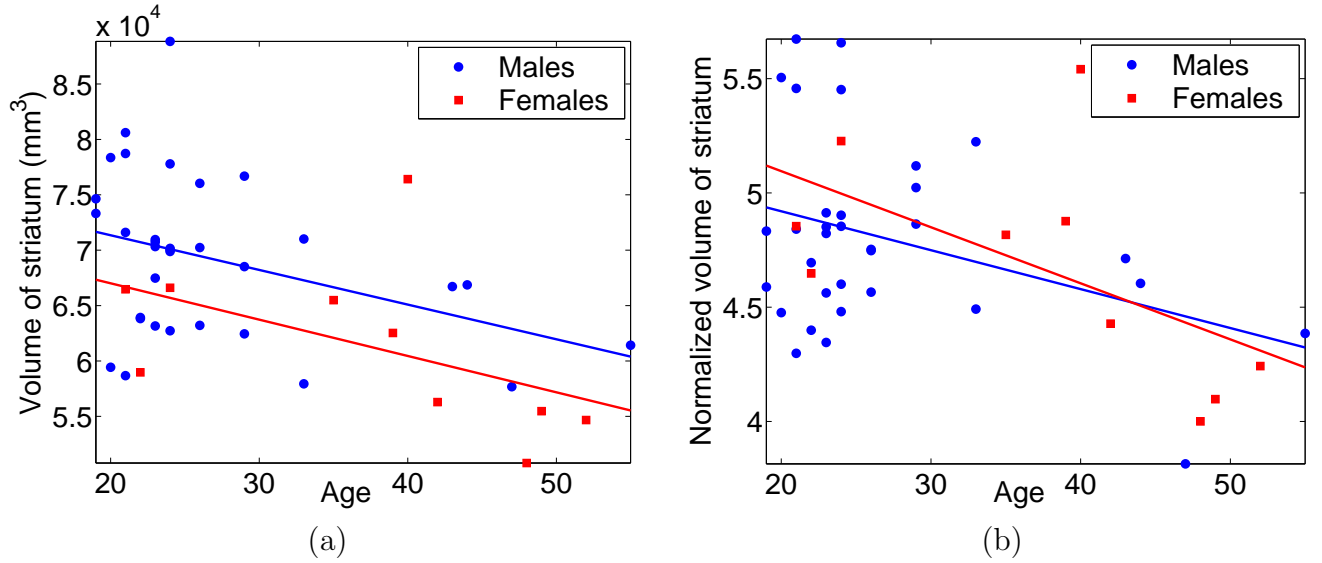
Figure 10: Results of the volume analysis. (a) The relation between the volume of the striatum and age ($c = -0.51$). (b) The relation between the normalized volume of the striatum and age ($c = -0.43$). The linear regression curves are plotted separately for males and females. (Publication III)

also for the whole brain. The correspondence was established for the striatum using first coarse alignment and then high-dimensional mapping. The shape analysis was performed based on the resulting point correspondence.

The volume of the striatum was normalized to the volume of the whole brain. The original and the normalized striatum volumes are plotted as a function of age in Fig. 10. The dependencies were tested using linear regression analysis. As a result, both the total brain volume ($p < 0.0005$) and age ($p < 0.005$) were statistically significant variables. Also, volumes of the right and left hemispheres were compared. No statistically significant difference between these volumes were detected.

The studies performed in Publication III showed that there were no statistically significant local shape differences between genders. On the other hand, the analysis with two age groups revealed statistically significant shape changes in aging (Fig. 11). The best correlation between age and a discriminant function was obtained using a combination of six PCA modes of shape variation. The correlation coefficient was 0.73. In the asymmetry study, the local shape analysis revealed that there were areas where the right and left parts were statistically significantly different.
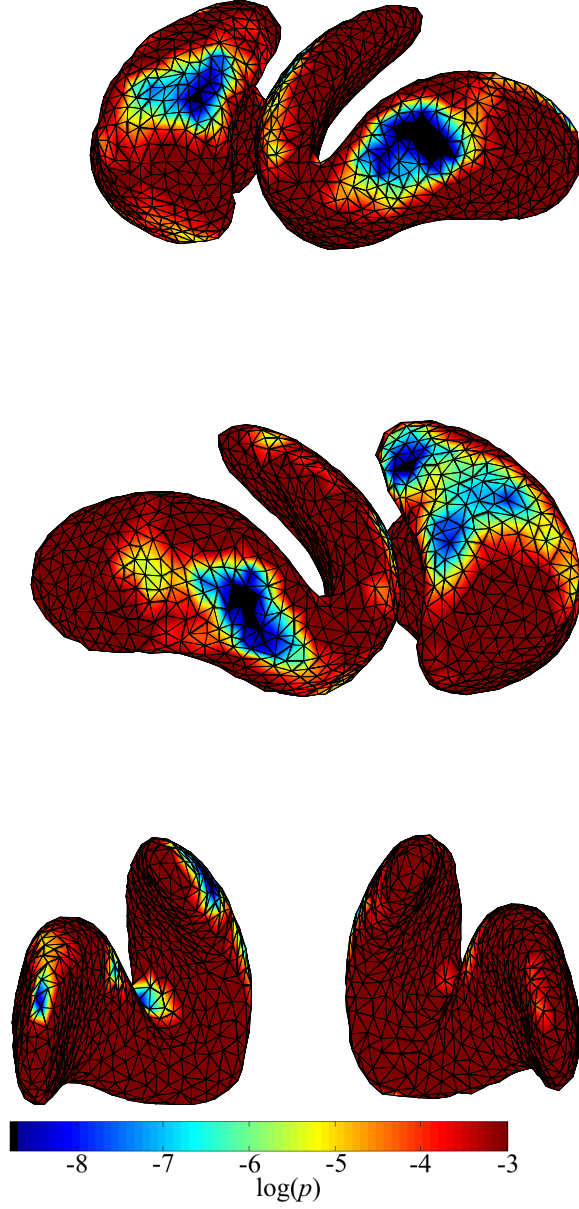
Figure 11: The *p*-values of the statistical tests of the local shape differences between the age groups (Wilcoxon rank sum test). The images show three views of the logarithm of the *p*-values on the surface of the striatum. The locations where statistically significant shape changes in aging were detected are shown in black color. The *p*-values larger than 0.05 were thresholded to 0.05, and they are shown in red color in the images. The *p*-value gives the probability that a chance has generated the differences observed between the two groups assuming identical distributions for the two groups. (Publication III)

6   Discussion

In this Thesis, methods that enable the modeling and utilization of prior knowledge on the shape and appearance of anatomical objects and on their variability were studied. This knowledge was obtained from the medical imaging data of a group of individuals. Different methods were studied to construct an accurate *a priori* model and to constrain the deformations in deformable model-based segmentation and non-rigid registration methods. In addition, shape analysis methods were studied and applied to the analysis of the shape of the striatum.

The model selection procedure is the simplest one of the methods studied. It does not require any correspondence between the database subjects. In the learning phase, a set of segmentations or registrations are done. Based on these results, a similarity measure is established from a set of features that describe the similarity between the database subjects and the target. On the other hand, the model selection can be done using only one similarity measure, such as NMI, in which case the learning phase is not required (Publication VII, Rohlfing et al. (2004a)). The model selection can be used with any existing deformable model-based segmentation or non-rigid registration algorithm without having to make any changes. The model selection procedure can also be adapted in several different ways. For example, it can be done either before or after segmentation or registration. Because the model selection can be used in many ways, it can also be adapted to the requirements of computation time. The model selection procedure allows more freedom to the problem than the deformable model-based methods usually do, since the same database can be used to segment targets with different topologies, if the corresponding topologies exist also in the database.

The adequate performance of the model selection procedure was proved. In Publication VII, it was shown that in the segmentation of 3-D MR images, the model selection procedure outperformed statistically significantly the random selection of an *a priori* model. Also in surface-based registration (Publications I and VI), the model selection improved the results considerably, as compared to the random selection of an *a priori* model.

Mean shape and appearance models are another relatively simply way to generate an accurate *a priori* model from the image databases for image segmentation and registration. The construction of the mean models usually requires the correspondence between the database subjects, although there exist methods in which this is not needed. However, the accuracy of the correspondence is not as important as, for example, in the statistical methods. Therefore, a reasonable mean model is usually obtained despite small errors in the correspondence. As with the model selection procedure, no changes have to be done to the segmentation or registration algorithm when the mean models are used as *a priori* models. Furthermore, the computational complexity is the same whether using the mean models or the random selection of an *a priori* model.

The efficacy of the mean models as *a priori* models was shown in different applications (Publications I, IV, and VI). In each study, the improvement in the accuracy, as compared to the use of individual subjects as *a priori* models, was observed. In Publications I and VI, the mean models and the model selection procedure gave approximately equally good accuracy. In Publication I, the combination of classifiers was also studied, and it provided the smallest registration error of the methods studied. However, the combination of classifiers is computationally much more expensive than the use of mean models. The results presented by Rohlfing et al. (2004a) were slightly different: the mean models outperformed the model selection. Therefore, it may be that the performance of the methods studied depends on the application and data.

Probabilistic and statistical methods provide a very interesting way to incorporate information on the variability of a population in segmentation and registration. However, there are some problems in the construction of these models which affect the registration and seg-

mentation performance. First, the correspondence between the database subjects has to be accurate. Otherwise, the model models not only the actual anatomical variability, but also the noise. Second, the databases are too small in most 3-D and 4-D models constructed. Therefore, the models do not include all the population-specific variability, and they cannot approximate accurately unseen examples of the population.

These problems were apparent also in the studies reported in Publications I, II, and VI. The databases were too small, and, therefore, the accuracy of the statistical methods was relatively modest, and the mean models and model selection gave better results. The probabilistic models studied were the non-parametric PDFs and probabilistic atlases. In these methods, Gaussian smoothing was performed to compensate for the small size of the database. Therefore, these models enabled larger variability than the database variability. In addition, in the probabilistic atlases, the correspondence was not needed, and the neighborhood information used in the atlases gave even more degrees of freedom to the model. Furthermore, the MAP framework was used in the segmentation with the probabilistic models. This was not as restricted as the segmentation using statistical models, in which only the shapes generated from the shape model were allowed. In the MAP framework, all shapes were possible, but they were weighted using the probabilistic model generated from the database. Consequently, the probabilistic methods, especially the probabilistic atlas, gave much better segmentation results than the statistical shape models (Publication II). It may be that after the size of the database is enlarged, and the models model the real population-specific variation, the statistical models outperform the probabilistic models. In addition, little bit different segmentation methods were used with the statistical and probabilistic models, which probably had some effect on the results.

The artificial enlargement of the database in the statistical shape models showed some potential (Publication V). However, it includes some drawbacks, too. One important feature, namely the specificity of the model, is lost in the artificial enlargement of the database. After this, the model may generate shapes that are not valid examples of the object studied. The artificial modes were utilized to approximate the shapes for which the point correspondence existed using the analytical solution. In this application, they produced good results. In segmentation, the problem is much more difficult. Analytical solutions do not exist but the optimal weights have to be searched using some optimization algorithm and criterion. Therefore, it has to be studied how applicable the artificially enlarged databases are in the real segmentation applications. However, errors in manual segmentations, especially in cardiac applications, make the evaluation of segmentation accuracy more difficult.

The studies with the sparse point sets (Publications I and VI) showed that surprisingly good registration accuracy can be obtained using just a few points from the surface of the skin. In these applications, *a priori* information available in an image database was crucial for good registrations. Especially for the internal organs, from which there were no data in the registration, the information on the anatomy and its variability has to be included in an *a priori* model. In the thorax study (Publication VI), the registration of the internal organs was a much more difficult problem because of the large anatomical variability and the distance from the skin. In this study, the statistical shape model (SDM) gave good results. This proved that these methods can learn the correlations between the objects. In Publication VI, a model that described the correlations between the surface points' coordinates and the size and location of the internal organs was learned from the database. This approach performed better than the other methods studied, which showed that simple methods may be very effective, especially if the database is small.

In the modeling of the shape of heart and in the segmentation of cardiac MR images, both SA and LA images were used simultaneously. This enabled accurate analysis of the ventricles in basal and valve level, and of the atria. This technique was proven to be very efficient in

segmentation (Publications II and IV). The comparison of the segmentation results obtained to the results presented in the literature is not straightforward since the surfaces used and the error measures are not identical. Nevertheless, the results presented in this Thesis are good, especially considering that the whole ventricles and also both atria were studied.

The shape analysis showed the power of the methods used. The age-related shape differences in the shape were so small that they were very difficult to notice by visually examining the individual shapes. However, the locations where the changes took place and quantitative information on the changes could be detected and visualized using the methods presented. The results of the volume analysis were similar to the results presented by Gunning-Dixon et al. (1998), Gunduz et al. (2002), and Brabec et al. (2003): the volume of the striatum decreases in aging.

The most obvious improvement for the methods presented would be the enlargement of the database. Especially in the probabilistic and statistical methods, this would improve the results. However, the results show that the size of the database is not as crucial for the model selection procedure, mean models, and combination of classifiers. Nevertheless, the performance of these methods would improve if the database was larger. Also in the shape analysis, the more there are subjects the more reliable the results are.

In Publication VI, separate model selections were performed for males and females, and it produced the best results in this study. A similar procedure could be utilized also with the mean models and probabilistic and statistical shape models, i.e., to construct own models for separate groups. This was tested in Publication VI for the mean models, but because of the small database it did not improve the results. The division into gender or age groups is trivial to perform. If other kind of groups are needed, it has to be defined how the division is done and which one of the models constructed should be used for the particular target subject. In these kind of questions, the model selection procedure can give answers. For example, only the most similar database models to the target could be searched from the database and used to construct a target-specific mean model. This way, the mean model would be very likely a valid example of the object studied, and this would produce a better *a priori* model for the particular target than a fixed mean model. In the statistical and probabilistic models, only the most similar database subjects to the target could be used to train the statistical/probabilistic model so that it would represent accurately the variability of the cases similar to the target. If the database is large, the segmentation or registration cannot be done using each database subject in the combination of classifiers. Therefore, one has to select which database models are used. The model selection procedure is a reasonable method for this problem.

7 Conclusions

In this Thesis, methods to model and utilize the prior knowledge available in medical image databases were studied and compared. The applications were the deformable model-based segmentation of MR images, the reconstruction of 3-D geometry from incomplete data, and the analysis of the shape of the striatum. The objective was to develop new methods for these applications, to study if the use of the prior knowledge from image databases improves the results in these applications, and to compare different methods proposed.

It was concluded that the image databases really improve the segmentation and registration accuracies in medical applications. However, it was observed that the size of the database was crucial in many methods. In many recent studies using statistical and probabilistic methods, especially in 3-D or 4-D, the problem has been the small size of the database. The anatomical variability cannot be modeled accurately from just 10–30 subjects. Therefore, larger databases have to be constructed, and this will probably improve the performance of the methods. Because of this problem, more and more interest and effort have been directed to the large international databases. For example, the database of an International Consortium for Brain Mapping (ICBM) contains images from 7000 subjects (Mazziotta et al., 2001). These kind of databases will be crucial for the successful application of the probabilistic and statistical models in registration and segmentation, and for efficient shape analysis.

When the problems related to the correspondence and the size of the database have been solved, the statistical and probabilistic methods may prove to be very efficient in many applications. Before this, simpler methods or methods which are not too sensitive to the size of the database can be used. For example, the model selection procedure, mean models, and combination of classifiers outperformed the statistical shape models in surface-based registration.

Automatic image analysis will play an important role in many medical applications as the number of images acquired yearly in hospitals increases and new imaging modalities provide novel information on the human body. Automatic methods studied in this Thesis decrease the workload of physicians and can give accurate and objective information for the physicians to aid in their diagnosis making.

8   Summary of publications

I Reconstruction of 3-D Head Geometry from Digitized Point Sets: an Evaluation Study

Different methods to reconstruct 3-D head geometry from digitized point sets were evaluated. The evaluated methods were the random selection of *a priori* models, model selection procedure, mean shape models, averaging of FFD registration results, and registration using SDM. The averaging of FFD registration results was the best method studied.

II Statistical Shape Model of Atria, Ventricles and Epicardium from Short- and Long-Axis MR Images

Different probabilistic and statistical shape models were constructed and used in the segmentation of cardiac structures. The models included both the ventricles and atria, and the epicardium. The models were constructed by combining the information in the short-axis (SA) and long-axis (LA) volumes. Probabilistic atlases produced the best segmentation accuracy.

III Age- and Gender-Related Shape Changes and Asymmetry of Striatum

The shape of striatum was studied by comparing the data of 43 healthy subjects. The comparison was done based on the spatial correspondence established for the database. Both volume and local shape changes were observed in aging. Asymmetries were found, too.

IV Segmentation of Cardiac Structures Simultaneously from Short- and Long-Axis MR Images

A mean appearance model was used as an *a priori* model in the segmentation of cardiac structures simultaneously from SA and LA MR volume images. The use of both SA and LA images improved the results as compared to the use of only SA images.

V Artificial Enlargement of a Training Set for Statistical Shape Models: Application to Cardiac Images

Methods to artificially enlarge the database for the construction of statistical shape models were developed and compared. It was shown that, in theory, such enlargement can notably improve the performance of the statistical shape model in segmentation.

VI Individualized Geometric Model from Unorganized 3-D Points: An Application to Thorax Modeling

A set of digitized points from the surface of the torso was used to construct a 3-D geometric model of the torso, lungs, and heart. The random selection of an *a priori* model, model selection procedure, mean models, and SDMs were compared. Also, the location and size of the internal organs were estimated based on the surface points' coordinates, and different model selections for males and females were studied. The best accuracy was obtained with the model selection procedure.

VII Model Library for Deformable Model-Based Segmentation of 3-D Brain MR-Images

The model selection procedure was introduced for the segmentation of volume images. Different similarity measures and regression analysis were used to select the best *a priori* model for the segmentation of brain MR volume images. Statistically significant improvement to the segmentation accuracy was obtained with the procedure presented.

Author's contribution

The original idea of the model selection for Publication VII was conceived by the instructor of this Thesis. The idea was further developed in Publications I and VI by the author. The author developed and implemented the methods for the model selection, and all the experiments in Publications I, VI, and VII were designed and conducted by the author. In Publications II and IV, the author designed and carried out approximately half of the experiments. Some of the methods were developed and implemented, and the experiments were partly realized by the author in Publication V. The idea for Publication III was discovered by the author and the co-authors. Methods for shape analysis were developed and implemented, and the study was mostly designed and completely conducted by the author. All the mean shape and appearance models, and the statistical shape models used in this Thesis were constructed by the author. The author implemented some of the rigid and affine registration methods used and made modifications to the non-rigid registration and deformable model-based segmentation methods developed by the instructor of this Thesis. Publications I, III, IV, VI, and VII were mostly written by the author, and Publications II and V were partly written by the author.

References

Archarya, R. and Menon, R. (1998). A Review of Biomedical Image Segmentation Techniques. In Singh, A., Goldgof, D., and Terzopoulos, D., editors, *Deformable Models in Medical Image Analysis*, pages 140–161. IEEE Computer Society, Los Alamitos, California, USA.

Ashburner, J. and Friston, K. (2000). Voxel-Based Morphometry - The Methods. *NeuroImage*, 11(6):805–821.

Ashburner, J., Hutton, C., Frackowiak, R., Johnsrude, I., Price, C., and Friston, K. (1998). Identifying Global Anatomical Differences: Deformation-Based Morphometry. *Human Brain Mapping*, 6(5-6):348–357.

Aylward, E., Sparks, B., Field, K., Yallapragada, V., Shpritz, B., Rosenblatt, A., Brandt, J., Gourley, L., Liang, K., Zhou, H., Margolis, R., and Ross, C. (2004). Onset and Rate of Striatal Atrophy in Preclinical Huntington Disease. *Neurology*, 63(1):66–72.

Barrick, T., Mackay, C., Prima, S., Maes, F., Vandermeulen, D., Crow, T., and Roberts, N. (2005). Automatic Analysis of Cerebral Asymmetry: An Exploratory Study of the Relationship Between Brain Torque and Planum Temporale Asymmetry. *NeuroImage*, 24(3):678–691.

Baumberg, A. and Hogg, D. (1995). An Adaptive Eigenshape Model. In Pycock, D, editor, *Proceedings of the 1995 British conference on Machine vision, BMVC '95*, volume 1, pages 87–96, Surrey, UK. BMVA Press.

Bhatia, K., Hajnal, J., Puri, B., Edwards, A., and Rueckert, D. (2004). Consistent Groupwise Non-Rigid Registration for Atlas Construction. In *ISBI*, pages 908–911. IEEE.

Blanton, R., Levitt, J., Peterson, J., Fadale, D., Sporty, M., Lee, M., To, D., Mormino, E., Thompson, P., McCracken, J., and Toga, A. (2004). Gender Differences in the Left Inferior Frontal Gyrus in Normal Children. *NeuroImage*, 22(2):626–636.

Bookstein, F. (1997). Shape and the Information in Medical Images: A Decade of the Morphometric Synthesis. *Computer Vision and Image Understanding*, 66(2):97–118.

Bouix, S., Pruessner, J., Collins, D., and Siddiqi, K. (2005). Hippocampal Shape Analysis Using Medial Surfaces. *NeuroImage*, 25(4):1077–1089.

Brabec, J., Krásenský, J., and Petrovický, P. (2003). Volumetry of Striatum and Pallidum in Man - Anatomy, Cytoarchitecture, Connections, MRI and Aging. *Sbor. lék.*, 104(1):13–65.

Brejl, M. and Sonka, M. (2000). Object Localization and Border Detection Criteria Design in Edge-Based Image Segmentation: Automated Learning from Examples. *IEEE Transactions on Medical Imaging*, 19(10):973–985.

Brett, A. and Taylor, C. (2000). A Method of Automated Landmark Generation for Automated 3D PDM Construction. *Image and Vision Computing*, 18(9):739–748.

Buchsbaum, M., Shihabuddin, L., Brickman, A., Miozzo, R., Prikryl, R., Shaw, R., and Davis, K. (2003). Caudate and Putamen Volumes in Good and Poor Outcome Patients with Schizophrenia. *Schizophrenia Research*, 64(1):53–62.

Buchsbaum, M., Yang, S., Hazlett, E., Siegel, Jr., B., Germans, M., Haznedar, M., O'Flaithbheartaigh, S., Wei, T., Silverman, J., and Siever, L. (1997). Ventricular Volume and Asymmetry in Schizotypal Personality Disorder and Schizophrenia Assessed with Magnetic Resonance Imaging. *Schizophrenia Research*, 27(1):45–53.

Caunce, A. and Taylor, C. (1999). Using Local Geometry to Build 3D Sulcal Models. In Kuba, A., Sámal, M., and Todd-Pokropek, A., editors, *IPMI*, volume 1613 of *Lecture Notes in Computer Science*, pages 196–209. Springer.

Chandrashekara, R., Rao, A., Sanchez-Ortiz, G., Mohiaddin, R., and Rueckert, D. (2003). Construction of a Statistical Model for Cardiac Motion Analysis Using Nonrigid Image Registration. In Taylor, C. J. and Noble, J. A., editors, *IPMI*, volume 2732 of *Lecture Notes in Computer Science*, pages 599–610. Springer.

Chen, M., Kanade, T., Pomerleau, D., and Rowley, H. (1999a). Anomaly Detection Through Registration. *Pattern Recognition*, 32(1):113–128.

Chen, M., Kanade, T., Pomerleau, D., and Schneider, J. (1999b). 3-D Deformable Registration of Medical Images Using a Statistical Atlas. In Taylor, C. and Colchester, A. C. F., editors, *MICCAI*, volume 1679 of *Lecture Notes in Computer Science*, pages 621–630. Springer.

Christensen, G., Joshi, S., and Miller, M. (1997). Volumetric Transformation of Brain Anatomy. *IEEE Transactions on Medical Imaging*, 16(6):864–877.

Cootes, T. and Taylor, C. (1995). Combining Point Distribution Models with Shape Models Based on Finite Element Analysis. *Image and Vision Computing*, 13(5):403–409.

Cootes, T. and Taylor, C. (2004). Statistical Models of Appearance for Computer Vision. Techinal report, University of Manchester.

Cootes, T., Taylor, C., Cooper, D., and Graham, J. (1995). Active Shape Models – Their Training and Application. *Computer Vision and Image Understanding*, 61(1):38–59.

Cootes, T., Taylor, C., and Lanitis, A. (1994). Multi-Resolution Search with Active Shape Models. In *ICPR*, volume 1, pages 610–612. IEEE.

Csernansky, J., Joshi, S., Wang, L., Haller, J., Gado, M., Miller, J., Grenander, U., and Miller, M. (1998). Hippocampal Morphometry in Schizophrenia by High Dimensional Brain Mapping. *Proceedings of the National Academy of Sciences of the United States of America*, 95(19):11406–11411.

Csernansky, J., Wang, L., Joshi, S., Ratnanather, J., and Miller, M. (2004). Computational Anatomy and Neuropsychiatric Disease: Probabilistic Assessment of Variation and Statistical Inference of Group Difference, Hemispheric Asymmetry, and Time-Dependent Change. *NeuroImage*, 23:S56–S68.

Csernansky, J., Wang, L., Swank, J., Miller, J., Gado, M., McKeel, D., Miller, M., and Morris, J. (2005). Preclinical Detection of Alzheimer's Disease: Hippocampal Shape and Volume Predict Dementia Onset in the Elderly. *NeuroImage*, 25(3):783–792.

Davatzikos, C. (1997). Spatial Transformation and Registration of Brain Images Using Elastically Deformable Models. *Computer Vision and Image Understanding*, 66(2):207–222.

Davatzikos, C., Tao, X., and Shen, D. (2003). Hierarchical Active Shape Models, Using the Wavelet Transform. *IEEE Transactions on Medical Imaging*, 22(3):414–423.

Davies, R., Twining, C., Cootes, T., Waterton, J., and Taylor, C. (2002). A Minimum Description Length Approach to Statistical Shape Modeling. *IEEE Transactions on Medical Imaging*, 21(5):525–537.

Dawant, B. and Zijdenbos, A. (2000). Image Segmentation. In Sonka, M. and Fitzpatrick, J., editors, *Handbook of Medical Imaging, Volume 2. Medical Imaging Processing and Analysis*, pages 71–127. SPIE Press, Belligngham, Washington, USA.

Deshmukh, A., Rosenbloom, M., De Rosa, E., Sullivan, E., and Pfefferbaum, A. (2005). Regional Striatal Volume Abnormalities in Schizophrenia: Effects of Comorbidity for Alcoholism, Recency of Alcoholic Drinking, and Antipsychotic Medication Type. *Schizophrenia Research*, In Press.

Duda, R. and Hart, P. (1973). *Pattern Classification and Scene Analysis*. John Wiley & Sons, New York.

Duta, N. and Sonka, M. (1998). Segmentation and Interpretation of MR Brain Images: An Improved Active Shape Model. *IEEE Transactions on Medical Imaging*, 17(6):1049–1062.

Fitzpatrick, J., Hill, D., and Maurer, Jr., C. (2000). Image Registration. In Sonka, M. and Fitzpatrick, J., editors, *Handbook of Medical Imaging, Volume 2: Medical Image Processing and Analysis*, pages 447–513. SPIE Press, Bellingham, Washington, USA.

Fitzpatrick, J., West, J., and Maurer, Jr., C. (1998). Predicting Error in Rigid-Body Point-Based Registration. *IEEE Transactions on Medical Imaging*, 17(5):694–702.

Fleute, M. and Lavallée, S. (1998). Building a Complete Surface Model from Sparse Data Using Statistical Shape Models: Application to Computer Assisted Knee Surgery. In III, W. M. W., Colchester, A. C. F., and Delp, S., editors, *MICCAI*, volume 1496 of *Lecture Notes in Computer Science*, pages 879–887. Springer.

Frangi, A., Rueckert, D., Schnabel, J., and Niessen, W. (2002). Automatic Construction of Multiple-Object Three-Dimensional Statistical Shape Models: Application to Cardiac Modeling. *IEEE Transactions on Medical Imaging*, 21(9):1151–1166.

Free, S., O'Higgins, P., Maudgil, D., Dryden, I., Lemieux, L., Fish, D., and Shorvon, S. (2001). Landmark-Based Morphometrics of the Normal Adult Brain Using MRI. *NeuroImage*, 13(5):801–813.

Gaser, C., Nenadic, I., Buchsbaum, B., Hazlett, E., and Buchsbaum, M. (2001). Deformation-Based Morphometry and Its Relation to Conventional Volumetry of Brain Lateral Ventricles in MRI. *NeuroImage*, 13(6):1140–1145.

Gaser, C., Volz, H.-P., Kiebel, S., Riehemann, S., and Sauer, H. (1999). Detecting Structural Changes in Whole Brain Based on Nonlinear Deformations - Application to Schizophrenia Research. *NeuroImage*, 10(2):107–113.

Gelman, A., Carlin, J., Stern, H., and Rubin, D. (1995). *Bayesian Data Analysis*. Chapman & Hall/CRC.

Gering, D. (2003). Diagonalized Nearest Neighbor Pattern Matching for Brain Tumor Segmentation. In Ellis, R. E. and Peters, T. M., editors, *MICCAI (2)*, volume 2879 of *Lecture Notes in Computer Science*, pages 670–677. Springer.

Golland, P., Grimson, W., and Kikinis, R. (1999). Statistical Shape Analysis Using Fixed Topology Skeletons: Corpus Callosum Study. In Kuba, A., Sámal, M., and Todd-Pokropek, A., editors, *IPMI*, volume 1613 of *Lecture Notes in Computer Science*, pages 382–387. Springer.

Golland, P., Grimson, W., Shenton, M., and Kikinis, R. (2005). Detection and Analysis of Statistical Differences in Anatomical Shape. *Medical Image Analysis*, 9(1):69–86.

Good, C., Johnsrude, I., Ashburner, J., Henson, R., Friston, K., and Frackowiak, R. (2001). A Voxel-Based Morphometric Study of Ageing in 465 Normal Adult Human Brains. *NeuroImage*, 14(1):21–36.

Goodall, C. (1991). Procrustes Methods in the Statistical Analysis of Shape. *Journal of the Royal Statistical Society. Series B.*, 53(2):285–339.

Gower, J. (1975). Generalized Procrustes Analysis. *Psychometrika*, 40:33–51.

Guimond, A., Meunier, J., and Thirion, J.-P. (2000). Average Brain Models. A Convergence Study. *Computer Vision and Image Understanding*, 77(2):192–210.

Gunduz, H., Wu, H., Ashtari, M., Bogerts, B., Crandall, D., Robinson, D., Alvir, J., Lieberman, J., Kane, J., and Bilder, R. (2002). Basal Ganglia Volumes in First-Episode Schizophrenia and Healthy Comparison Subjects. *Biological Psychiatry*, 51(10):801–808.

Gunning-Dixon, F., Head, D., McQuain, J., Acker, J., and Raz, N. (1998). Differential Aging of the Human Striatum: A Prospective MR Imaging Study. *American Journal of Neuroradiology*, 19(8):1501–1507.

Hawkes, D. (2001). Registration Methodology: Introduction. In Hajnal, J., Hill, D., and Hawkes, D., editors, *Medical Image Registration*, pages 11–38. CRC Press, USA.

Hill, A., Taylor, C., and Brett, A. (2000). A Framework for Automatic Landmark Identification Using a New Method of Nonrigid Correspondence. *IEEE Transactions on Pattern Analysis and Machine Intelligence*, 22(3):241–251.

Hill, D. and Batchelor, P. (2001). Registration Methodology: Concepts and Algorithms. In Hajnal, J., Hill, D., and Hawkes, D., editors, *Medical Image Registration*, pages 39–70. CRC Press, USA.

Hollander, E., Anagnostou, E., Chaplin, W., Esposito, K., Haznedar, M., Licalzi, E., Wasserman, S., Soorya, L., and Buchsbaum, M. (2005). Striatal Volume on Magnetic Resonance Imaging and Repetitive Behaviors in Autism. *Biological Psychiatry*, 58(3):226–232.

Hyvärinen, A., Karhunen, J., and Oja, E. (2001). *Independent Component Analysis*. John Wiley & Sons.

Joshi, S., Davis, B., Jomier, M., and Gerig, G. (2004). Unbiased Diffeomorphic Atlas Construction for Computational Anatomy. *NeuroImage*, 23:S151–S160.

Joshi, S., Pizer, S., Fletcher, P., Yushkevich, P., Thall, A., and Marron, J. (2002). Multiscale Deformable Models Segmentation and Statistical Shape Analysis Using Medial Descriptions. *IEEE Transactions on Medical Imaging*, 21(5):538–550.

Kass, M., Witkin, A., and Terzopoulos, D. (1987). Snakes: Active Contour Models. *International Journal of Computer Vision*, 1(4):321–331.

Kaus, M., Pekar, V., Lorenz, C., Truyen, R., Lobregt, S., and Weese, J. (2003a). Automated 3-D PDM Construction from Segmented Images Using Deformable Models. *IEEE Transactions on Medical Imaging*, 22(8):1005–1013.

Kaus, M., von Pekar, J., Niessen, W., and Pekar, V. (2003b). Automated Segmentation of the Left Ventricle in Cardiac MRI. In Ellis, R. E. and Peters, T. M., editors, *MICCAI (1)*, volume 2878 of *Lecture Notes in Computer Science*, pages 432–439. Springer.

Kelemen, A., Székely, G., and Gerig, G. (1999). Elastic Model-Based Segmentation of 3-D Neuroradiological Data Sets. *IEEE Transactions on Medical Imaging*, 18(10):828–839.

Koikkalainen, J. and Lötjönen, J. (2004). Image Segmentation with the Combination of the PCA- and ICA-Based Modes of Shape Variation. In *ISBI*, pages 149–152. IEEE.

Kotcheff, A. and Taylor, C. (1998). Automatic Construction of Eigenshape Models by Direct Optimization. *Medical Image Analysis*, 2(4):303–314.

Kovalev, V., Kruggel, F., and von Cramon, D. (2003). Gender and Age Effects in Structural Brain Asymmetry as Measured by MRI Texture Analysis. *NeuroImage*, 19(3):895–905.

Lacerda, A., Nicoletti, M., Brambilla, P., Sassi, R., Mallinger, A., Frank, E., Kupfer, D., Keshavan, M., and Soares, J. (2003). Anatomical MRI Study of Basal Ganglia in Major Depressive Disorder. *Psychiatry Research: Neuroimaging*, 124(3):129–140.

Le Goualher, G., Argenti, A., Duyme, M., Baaré, W., Hulshoff Pol, H., Boomsma, D., Zouaoui, A., Barillot, C., and Evans, A. (2000). Statistical Sulcal Shape Comparisons: Application to the Detection of Genetic Encoding of the Central Sulcus Shape. *NeuroImage*, 11(5):564–573.

Lee, J.-M., Kim, S., Jang, D., Ha, T., Kim, J.-J., Kim, I., Kwon, J., and Kim, S. (2004). Deformable Model with Surface Registration for Hippocampal Shape Deformity Analysis in Schizophrenia. *NeuroImage*, 22(2):831–840.

Lelieveldt, B., Üzümcü, M., van der Geest, R., Reiber, J., and Sonka, M. (2003). Multi-View Active Appearance Models for Consistent Segmentation of Multiple Standard Views: Application to Long and Short-Axis Cardiac MR Images. In Lemke, H. U., Vannier, M. W., Inamura, K., Farman, A. G., Doi, K., and Reiber, J. H. C., editors, *CARS*, volume 1256 of *International Congress Series*, pages 1141–1146. Elsevier.

Leventon, M., Grimson, W., and Faugeras, O. (2000). Statistical Shape Influence in Geodesic Active Contours. In *CVPR*, pages 1316–1323. IEEE Computer Society.

Levitt, J., McCarley, R., Dickey, C., Voglmaier, M., Niznikiewicz, M., Seidman, L., Hirayasu, Y., Ciszewski, A., Kikinis, R., Jolesz, F., and Shenton, M. (2002). MRI Study of Caudate Nucleus Volume and Its Cognitive Correlates in Neuroleptic-Naive Patients with Schizotypal Personality Disorder. *American Journal of Psychiatry*, 159(7):1190–1197.

Levitt, J., Westin, C., Nestor, P., Estepar, R., Dickey, C., Voglmaier, M., Seidman, L., Kikinis, R., Jolesz, F., McCarley, R., and Shenton, M. (2004). Shape of Caudate Nucleus and Its Cognitive Correlates in Neuroleptic-Naive Schizotypal Personality Disorder. *Biological Psychiatry*, 55(2):177–184.

Liu, R., Lemieux, L., Bell, G., Sisodiya, S., Shorvon, S., Sander, J., and Duncan, J. (2003). A Longitudinal Study of Brain Morphometrics Using Quantitative Magnetic Resonance Imaging and Difference Image Analysis. *NeuroImage*, 20(1):22–33.

Loeckx, D., Maes, F., Vandermeulen, D., and Suetens, P. (2003). Temporal Subtraction of Thorax CR Images Using a Statistical Deformation Model. *IEEE Transactions on Medical Imaging*, 22(11):1490–1504.

Lorenz, C. and Krahnstöver, N. (2000). Generation of Point-Based 3D Statistical Shape Models for Anatomical Objects. *Computer Vision and Image Understanding*, 77(9):175–191.

Lorenzo-Valdés, M., Sanchez-Ortiz, G., Elkington, A., Mohiaddin, R., and Rueckert, D. (2004). Segmentation of 4D Cardiac MR Images Using a Probabilistic Atlas and the EM Algorithm. *Medical Image Analysis*, 8(3):255–265.

Lorenzo-Valdés, M., Sanchez-Ortiz, G., Mohiaddin, R., and Rueckert, D. (2002). Atlas-Based Segmentation and Tracking of 3D Cardiac MR Images Using Non-Rigid Registration. In Dohi, T. and Kikinis, R., editors, *MICCAI (1)*, volume 2488 of *Lecture Notes in Computer Science*, pages 642–650. Springer.

Lötjönen, J. and Mäkelä, T. (2001). Elastic Matching Using a Deformation Sphere. In Niessen, W. J. and Viergever, M. A., editors, *MICCAI*, volume 2208 of *Lecture Notes in Computer Science*, pages 541–548. Springer.

Lötjönen, J., Pollari, M., Kivistö, S., and Lauerma, K. (2005). Correction of Motion Artifacts from Cardiac Cine Magnetic Resonance Images. *Academic Radiology*, 12(10):1273–1284.

Lötjönen, J., Reissman, P.-J., Magnin, I., and Katila, T. (1999). Model Extraction from Magnetic Resonance Volume Data Using the Deformable Pyramid. *Medical Image Analysis*, 3(4):387–406.

Magnin, J.-F., Rivière, D., Cachia, A., Duchesnay, E., Cointepas, Y., Papadopoulos-Orfanos, D., Collins, D., Evans, A., and J.Régis (2004). Object-Based Morphometry of the Cerebral Cortex. *IEEE Transactions on Medical Imaging*, 23(8):968–982.

Maintz, J. and Viergever, M. (1998). A Survey of Medical Image Registration. *Medical Image Analysis*, 2(1):1–36.

Mäkelä, T., Clarysse, P., Sipilä, O., Pauna, N., Pham, Q., Katila, T., and Magnin, I. (2002). A Review of Cardiac Image Registration Methods. *IEEE Transactions on Medical Imaging*, 21(9):1011–1021.

Marsland, S., Twining, C., and Taylor, C. (2003). Groupwise Non-Rigid Registration Using Polyharmonic Clamped-Plate Splines. In Ellis, R. E. and Peters, T. M., editors, *MICCAI (2)*, volume 2879 of *Lecture Notes in Computer Science*, pages 771–779. Springer.

Mazziotta, J., Toga, A., Evans, A., ans J. Lancaster, P. F., Zilles, K., Woods, R., Paus, T., Simpson, G., Pike, B., Holmes, C., Collins, L., Thompson, P., MacDonald, D., Iacoboni, M., Schormann, T., Amunts, K., Palomero-Gallagher, N., Geyer, S., Parsons, L., Narr, K., Kabani, N., Goualher, G. L., Boomsma, D., Cannon, T., Kawashima, R., and Mazoyer, B. (2001). A Probabilistic Atlas and Reference System for the Human Brain: International Consortium for Brain Mapping (ICBM). *Philosophical Transactions of the Royal Society of London, Series B: Biological Sciences.*, 356(1412):1293–1322.

McInerney, T. and Terzopoulos, D. (1996). Deformable Models in Medical Image Analysis: A Survey. *Medical Image Analysis*, 1(2):91–108.

Meier, D. and Fisher, E. (2002). Parameter Space Warping: Shape-Based Correspondence between Morpholigically Different Objects. *IEEE Transactions on Medical Imaging*, 21(1):31–47.

Mitchell, S., Bosch, J., Lelieveldt, B., van der Geest, R., Reiber, J., and Sonka, M. (2002). 3-D Active Appearance Models: Segmentation of Cardiac MR and Ultrasound Images. *IEEE Transactions on Medical Imaging*, 21(9):1167–1178.

Mitchell, S., Lelieveldt, B., van der Geest, R., Bosch, J., Reiber, J., and Sonka, M. (2001). Multistage Hybrid Active Appearance Model Matching: Segmentation of Left and Right Ventricles in Cardiac MR Images. *IEEE Transactions on Medical Imaging*, 20(5):415–423.

Narr, K., Thompson, P., Szeszko, P., Robinson, D., Jang, S., Woods, R., Kim, S., Hayashi, K., Asunction, D., Toga, A., and Bilder, R. (2004). Regional Specificity of Hippocampal Volume Reductions in First-Episode Schizophrenia. *NeuroImage*, 21(4):1563–1575.

Neumann, A. and Lorenz, C. (1998). Statistical Shape Model Based Segmentation of Medical Images. *Computerized Medical Imaging and Graphics*, 22(2):133–143.

Oost, C., Lelieveldt, B., Üzümcü, M., Lamb, H., Reiber, J., and Sonka, M. (2003). Multi-View Active Appearance Models: Application to X-Ray LV Angiography and Cardiac MRI. In Taylor, C. J. and Noble, J. A., editors, *IPMI*, volume 2732 of *Lecture Notes in Computer Science*, pages 234–245. Springer.

Ordas, S., Boisrobert, L., Bossa, M., Olmos, S., Frangi, A., Huguet, M., and Laucelli, M. (2004). Grid-Enabled Automatic Construction of a Two-Chamber Cardiac PDM from a Large Database of Dynamic 3D Shapes. In *ISBI*, pages 416–419. IEEE.

Paragios, N. (2003). A Level Set Approach for Shape-Driven Segmentation and Tracking of the Left Ventricle. *IEEE Transactions on Medical Imaging*, 22(6):773–776.

Park, H., Bland, P., and Meyer, C. (2003). Construction of an Abdominal Probabilistic Atlas and Its Application in Segmentation. *IEEE Transactions on Medical Imaging*, 22(4):483–492.

Park, H.-J., Westin, C.-F., Kubicki, M., Maier, S., Niznikiewicz, M., Baer, A., Frumin, M., Kikinis, R., Jolesz, F., McCarley, R., and Shenton, M. (2004). White Matter Hemisphere Asymmetries in Healthy Subjects and in Schizophrenia: A Diffusion Tensor MRI Study. *NeuroImage*, 23(1):213–223.

Perperidis, D., Lorezo-Valdés, M., Chandrashekara, R., Rao, A., Mohiaddin, R., Sanchez-Ortiz, G., and Rueckert, D. (2004). Building a 4D Atlas of the Cardiac Anatomy and Motion Using MR Imaging. In *ISBI*, pages 412–415. IEEE.

Perperidis, D., Mohiaddin, R., and Rueckert, D. (2005). Spatio-Temporal Free-Form Registration of Cardiac MR Image Sequences. *Medical Image Analysis*, 9(5):441–456.

Pizer, S., Fritsch, D., Yushkevich, P., Johnson, V., and Chaney, E. (1999). Segmentation, Registration, and Measurement of Shape Variation via Image Object Shape. *IEEE Transactions on Medical Imaging*, 18(10):851–865.

Posener, J., Wang, L., Price, J., Gado, M., Province, M., Miller, M., Babb, C., and Csernansky, J. (2003). High-Dimensional Mapping of the Hippocampus in Depression. *American Journal of Psychiatry*, 160(1):83–89.

Pujol, J., López-Sala, A., Deus, J., Cardoner, N., Sebastián-Gallés, N., Conesa, G., and Capdevila, A. (2002). The Lateral Asymmetry of the Human Brain Studied by Volumetric Magnetic Resonance Imaging. *NeuroImage*, 17(2):670–679.

Rao, A., Sanchez-Ortiz, G., Chandrashekara, R., Lorenzo-Valdés, M., Mohiaddin, R., and Rueckert, D. (2003). Construction of a Cardiac Motion Atlas from MR Using Non-Rigid Registration. In Magnin, I. E., Montagnat, J., Clarysse, P., Nenonen, J., and Katila, T., editors, *FIMH*, volume 2674 of *Lecture Notes in Computer Science*, pages 141–150. Springer.

Raz, N., Gunning-Dixon, F., Head, D., Williamson, A., and Acker, J. (2001). Age and Sex Differences in the Cerebellum and the Ventral Pons: A Prospective MR Study of Healthy Adults. *American Journal of Neuroradiology*, 22(6):1161–1167.

Resnick, S., Goldszal, A., Davatzikos, C., Golski, S., Kraut, M., Metter, E., Bryan, R., and Zonderman, A. (2000). One-year Age Changes in MRI Brain Volumes in Older Adults. *Cerebral Cortex*, 10(5):464–472.

Rogowska, J. (2001). Overview and Fundamentals of Medical Image Segmentation. In Bankman, I., editor, *Handbook of Medical Imaging: Processing and Analysis*, pages 69–85. Academic Press, USA.

Rohlfing, T., Brandt, R., Maurer, Jr., C., and Menzel, R. (2001). Bee Brains, B-splines and Computational Democracy: Generating an Average Shape Atlas. In *IEEE Workshop on Mathematical Methods in Biomedical Image Analysis (MMBIA 2001)*, pages 187–194.

Rohlfing, T., Brandt, R., Menzel, R., and Maurer, Jr., C. (2004a). Evaluation of Atlas Selection Strategies for Atlas-Based Image Segmentation with Application to Confocal Microscopy Images of Bee Brains. *NeuroImage*, 21(4):1428–1442.

Rohlfing, T., Russakoff, D., and Maurer, Jr., C. (2004b). Performance-Based Classifier Combination in Atlas-Based Image Segmentation Using Expectation-Maximization Parameter Estimation. *IEEE Transactions on Medical Imaging*, 23(8):983–994.

Royackkers, N., Desvignes, M., Fawal, H., and Revenu, M. (1999). Detection and Statistical Analysis of Human Cortical Sulci. *NeuroImage*, 10(6):625–641.

Rueckert, D. (2001). Nonrigid Registration: Concepts, Algorithms, and Applications. In Hajnal, J., Hill, D., and Hawkes, D., editors, *Medical Image Registration*, pages 281–301. CRC Press, USA.

Rueckert, D., Frangi, A., and Schnabel, J. (2003). Automatic Construction of 3-D Statistical Deformation Models of the Brain Using Nonrigid Registration. *IEEE Transactions on Medical Imaging*, 22(8):1014–1025.

Rueckert, D., Sonoda, L., Hayes, C., Hill, D., Leach, M., and Hawkes, D. (1999). Nonrigid Registration Using Free-Form Deformations: Application to Breast MR Images. *IEEE Transactions on Medical Imaging*, 18(8):712–721.

Rusch, B., Abercrombie, H., Oakes, T., Schaefer, S., and Davidson, R. (2001). Hippocampal Morphometry in Depressed Patients and Control Subjects: Relations to Anxiety Symptoms. *Biological Psychiatry*, 50(12):960–964.

Sampath, Y., Vetsa, K., Styner, M., Pizer, S., Lieberman, J., and Gerig, G. (2003). Caudate Shape Discrimination in Schizophrenia Using Template-Free Non-Parametric Tests. In Ellis, R. E. and Peters, T. M., editors, *MICCAI (2)*, volume 2879 of *Lecture Notes in Computer Science*, pages 661–669. Springer.

Sclaroff, S. and Isidoro, J. (1998). Active Blobs. In *Proc. International Conference on Computer Vision (ICCV'98)*, pages 1146–1153.

Sederberg, T. and Parry, S. (1986). Free-Form Deformation of Solid Geometric Models. In *Proc. International Conference on Computer Graphics and Interactive Techniques (SIGGRAPH'86)*, pages 151–160.

Shen, D., Herskovits, E., and Davatzikos, C. (2001). Adaptive-Focus Statistical Shape Model for Segmentation and Shape Modeling of 3-D Brain Structures. *IEEE Transactions on Medical Imaging*, 20(4):257–270.

Shenton, M., Gerig, G., McCarley, R., Székely, G., and Kikinis, R. (2002). Amygdala-Hippocampal Shape Differences in Schizophrenia: The Application of 3D Shape Models to Volumetric MR Data. *Psychiatry Research: Neuroimaging*, 115(1-2):15–35.

Shihabuddin, L., Buchsbaum, M., Hazlett, E., Silverman, J., New, A., Brickman, A., Mitropoulou, V., Nunn, M., Fleischman, M., Tang, C., and Siever, L. (2001). Striatal Size and Relative Glucose Metabolic Rate in Schizotypal Personality Disorder and Schizophrenia. *Archives of General Psychiatry*, 58(9):877–884.

Sluimer, I., Prokop, M., and van Ginneken, B. (2005). Toward Automated Segmentation of the Pathological Lung in CT. *IEEE Transactions on Medical Imaging*, 24(8):1025–1038.

Staib, L. and Duncan, J. (1992). Boundary Finding with Parametrically Deformable Models. *IEEE Transactions on Pattern Analysis and Machine Intelligence*, 14(11):1061–1075.

Staib, L. and Duncan, J. (1996). Model-Based Deformable Surface Finding for Medical Images. *IEEE Transactions on Medical Imaging*, 15(5):720–731.

Stegmann, M. and Larsen, R. (2003). Motion-Compensation of Cardiac Perfusion MRI Using a Statistical Texture Ensemble. In Magnin, I. E., Montagnat, J., Clarysse, P., Nenonen, J., and Katila, T., editors, *FIMH*, volume 2674 of *Lecture Notes in Computer Science*, pages 151–161. Springer.

Strakowski, S., DelBello, M., Zimmerman, M., Getz, G., Mills, N., Ret, J., Shear, P., and Adler, C. (2002). Ventricular and Periventricular Structural Volumes in First- Versus Multiple-Episode Bipolar Disorder. *American Journal of Psychiatry*, 159(11):1841–1847.

Studholme, C. (2003). Simultaneous Population Based Image Alignment for Template Free Spatial Normalisation of Brain Anatomy. In Gee, J. C., Maintz, J. B. A., and Vannier, M. W., editors, *WBIR*, volume 2717 of *Lecture Notes in Computer Science*, pages 81–90. Springer.

Studholme, C., Hill, D., and Hawkes, D. (1999). An Overlap Invariant Entropy Measure of 3D Medical Image Alignment. *Pattern Recognition*, 32(1):71–86.

Styner, M., Gerig, G., Lieberman, J., Jones, D., and Weinberger, D. (2003). Statistical Shape Analysis of Neuroanatomical Structures Based on Medial Models. *Medical Image Analysis*, 7(3):207–220.

Styner, M., Lieberman, J., McClure, R., Weinberger, D., Jones, D., and Gerig, G. (2005). Morphometric Analysis of Lateral Ventricles in Schizophrenia and Healthy Controls Regarding Genetic and Disease-Specific Factors. *Proceedings of the National Academy Sciences of the United States of America*, 102(13):4872–4877.

Styner, M., Lieberman, J., Pantazis, D., and Gerig, G. (2004). Boundary and Medial Shape Analysis of the Hippocampus in Schizophrenia. *Medical Image Analysis*, 8(3):197–203.

Subsol, G., Thirion, J.-P., and Ayache, N. (1998). A Scheme for Automatically Building Three-Dimensional Morphometric Anatomical Atlases: Application to a Skull Atlas. *Medical Image Analysis*, 2(1):37–60.

Suri, J. (2000). Computer Vision, Pattern Recognition and Image Processing in Left Ventricle Segmentation: The Last 50 Years. *Pattern Analysis & Applications*, 3(3):209–242.

Székely, G., Kelemen, A., Brechbühler, C., and Gerig, G. (1996). Segmentation of 2-D and 3-D Objects from MRI Volume Data Using Constrained Elastic Deformations or Flexible Fourier Contour and Surface Models. *Medical Image Analysis*, 1(1):19–34.

Tagare, H., O'Shea, D., and Rangarajan, A. (1995). A Geometric Criterion for Shape-based Non-rigid Correspondence. In *Proc. Fifth International Conference on Computer Vision (ICCV'95)*, pages 434–439, Cambridge, USA.

Tepest, R., Wang, L., Miller, M., Falkai, P., and Csernansky, J. (2003). Hippocampal Deformities in the Unaffected Siblings of Schizophrenia Subjects. *Biological Psychiatry*, 54(11):1234–1240.

Thirion, J.-P., Prima, S., Subsol, G., and Roberts, N. (2000). Statistical Analysis of Normal and Abnormal Dissymmetry in Volumetric Medical Images. *Medical Image Analysis*, 4(2):111–121.

Thodberg, H. (2003). Minimum Description Length Shape and Appearance Models. In Taylor, C. J. and Noble, J. A., editors, *IPMI*, volume 2732 of *Lecture Notes in Computer Science*, pages 51–62. Springer.

Thompson, P., Hayashi, K., Sowell, E., Gogtay, N., Giedd, J., Rapoport, J., de Zubicaray, G., Janke, A., Rose, S., Semple, J., Doddrell, D., Wang, Y., van Erp, T., Cannon, T., and Toga, A. (2004). Mapping Cortical Change in Alzheimer's Disease, Brain Development, and Schizophrenia. *NeuroImage*, 23:S2–S18.

Thompson, P., Mega, M., and Toga, A. (1997). Detection, Visualization and Animation of Abnormal Anatomic Structure with a Deformable Probabilistic Brain Atlas Based on Random Vector Field Transformations. *Medical Image Analysis*, 1(4):271–294.

Thompson, P. and Toga, A. (2002). A Framework for Computational Anatomy. *Computing and Visualization in Science*, 5(1):13–34.

Tsai, A., Wells, W., Tempany, D., Grimson, W., and Willsky, A. (2003). Coupled Multi-shape Model and Mutual Information for Medical Image Segmentation. In Taylor, C. J. and Noble, J. A., editors, *IPMI*, volume 2732 of *Lecture Notes in Computer Science*, pages 185–197. Springer.

Üzümcü, M., Frangi, A., Sonka, M., Reiber, J., and Lelieveldt, B. (2003). ICA vs. PCA Active Appearance Models: Application to Cardiac MR Segmentation. In *Proc. Medical Image Computing & Computer-Assisted Intervention (MICCAI'03)*, pages 451–458, Montréal, Canada.

van Assen, H., Danilouchkine, M., Frangi, A., Ordas, S., Westenberg, J., Reiber, J., and Lelieveldt, B. (2005). SPASM: Segmentation of Sparse and Arbitrarily Oriented Cardiac MRI Data Using a 3D-ASM. In Frangi, A. F., Radeva, P., Santos, A., and Hernandez, M., editors, *FIMH*, volume 3504 of *Lecture Notes in Computer Science*, pages 33–43. Springer.

van Ginneken, B., Frangi, A., Staal, J., ter Haar Romeny, B., and Viergever, M. (2002). Active Shape Model Segmentation with Optimal Features. *IEEE Transactions on Medical Imaging*, 21(8):924–933.

van Haren, N., Picchioni, M., McDonald, C., Marshall, N., Davis, N., Ribchester, T., Hulshoff Pol, H., Sharma, T., Sham, P., Kahn, R., and Murray, R. (2004). A Controlled Study of Brain Structure in Monozygotic Twins Concordant and Discordant for Schizophrenia. *Biological Psychiatry*, 56(6):454–461.

Van Leemput, K., Maes, F., Vandermeulen, D., Colchester, A., and Suetens, P. (2001). Automated Segmentation of Multiple Sclerosis Lesions by Model Outlier Detection. *IEEE Transactions on Medical Imaging*, 20(8):677–688.

Van Leemput, K., Maes, F., Vandermeulen, D., and Suetens, P. (1999). Automated Model-Based Tissue Classification of MR Images of the Brain. *IEEE Transactions on Medical Imaging*, 18(10):897–908.

van't Ent, D., de Munck, J., and Kaas, A. (2001). A Fast Method to Derive Realistic BEM Models for E/MEG Source Reconstruction. *IEEE Transactions on Biomedical Engineering*, 48(12):1434–1443.

Wang, L., Joshi, S., Miller, M., and Csernansky, J. (2001). Statistical Analysis of Hippocampal Asymmetry in Schizophrenia. *NeuroImage*, 14(3):531–545.

Wang, L., Swank, J., Glick, I., Gado, M., Miller, M., Morris, J., and Csernansky, J. (2003). Changes in Hippocampal Volume and Shape across Time Distinguish Dementia of the Alzheimer Type from Healthy Aging. *NeuroImage*, 20(2):667–682.

Wang, Y. and Staib, L. (2000a). Boundary Finding with Prior Shape and Smoothness Models. *IEEE Transactions on Pattern Analysis and Machine Intelligence*, 22(7):738–743.

Wang, Y. and Staib, L. (2000b). Physical Model-Based Non-Rigid Registration Incorporating Statistical Shape Information. *Medical Image Analysis*, 4(1):7–20.

Warfield, S., Zou, K., and Wells, W. (2002). Validation of Image Segmentation and Expert Quality with an Expectation-Maximization Algorithm. In Dohi, T. and Kikinis, R., editors, *MICCAI (1)*, volume 2488 of *Lecture Notes in Computer Science*, pages 298–306. Springer.

Watkins, K., Paus, T., Lerch, J., Zijdenbos, A., Collins, D., Neelin, P., Taylor, J., Worsley, K., and Evans, A. (2001). Structural Asymmetries in the Human Brain: A Voxel-Based Statistical Analysis of 142 MRI Scans. *Cerebral Cortex*, 11(9):868–877.

Wörz, S. and Rohr, K. (2003). Localization of Anatomical Point Landmarks in 3D Medical Images by Fitting 3D Parametric Intensity Models. In Taylor, C. J. and Noble, J. A., editors, *IPMI*, volume 2732 of *Lecture Notes in Computer Science*, pages 76–88. Springer.

Xu, C., Pham, D., and Prince, J. (2000a). Image Segmentation Using Deformable Models. In Sonka, M. and Fitzpatrick, J., editors, *Handbook of Medical Imaging, Volume 2. Medical Imaging Processing and Analysis*, pages 129–174. SPIE Press, Belligngham, Washington, USA.

Xu, J., Kobayashi, S., Yamaguchi, S., Iijima, K., Okada, K., and Yamashita, K. (2000b). Gender Effects on Age-Related Changes in Brain Structure. *American Journal of Neuroradiology*, 21(1):112–118.

Yang, J. and Duncan, J. (2003). 3D Image Segmentation of Deformable Objects with Shape-Appearance Joint Prior Models. In Ellis, R. E. and Peters, T. M., editors, *MICCAI (1)*, volume 2878 of *Lecture Notes in Computer Science*, pages 573–580. Springer.

Yang, J., Staib, L., and Duncan, J. (2003). Neighbor-Constrained Segmentation with 3D Deformable Models. In Taylor, C. J. and Noble, J. A., editors, *IPMI*, volume 2732 of *Lecture Notes in Computer Science*, pages 198–209. Springer.

Yang, J., Tagare, H., Staib, L., and Duncan, J. (2004). Segmentation of 3D Deformable Objects with Level Set Based Prior Models. In *ISBI*, pages 85–88. IEEE.